concentration was detected in the small intestinal epithelium. On the other hand, a small amount of NK012 was found in the feces and NK012 was weakly and uniformly distributed in the mucosal interstitium. A portion of SN-38 converted from CPT-11 undergoes subsequent conjugation as induced by UDP-glucuronyltransferase to form SN-38 β-glucuronide (SN-38-Glu) [27]. CPT-11, SN-38, and SN-38-Glu are excreted into the bile and then reach the small intestinal lumen [27,28]. SN-38-Glu is deconjugated in the cecum and colon to regenerate SN-38 through bacterial β-glucuronidase [29]. In our study, CPT-11 was excreted into feces much more than NK012 and a high CPT-11 concentration was detected in the small intestinal epithelium. It is speculated that the highly excreted CPT-11 is reabsorbed in the small intestinal epithelium and converted to SN-38 to damage the intestinal mucosa. On the other hand, NK012 was uniformly distributed in the mucosal interstitium at a lower concentration and this is suggested to be related to the less mucosal damage and diarrhea than those induced by CPT-11, although NK012 was observed for longer period than CPT-11 [30]. Very recently we also found that NK012/S-1, a dihydropyrimidine dehydrogenase inhibitory fluoropyrimidine, showed a significantly higher antitumor activity with less intestinal damage than CPT-11/S-1, one of the promising regimens against non SCLC, advanced colorectal cancer, and metastatic advanced gastric cancer [31].

3.3. Renal cell cancer (RCC)

The results of chemotherapy in RCCs have been disappointing, as indicated by the low response rate. However, clinical trials using an antimetabolite, gemcitabine-containing regimens have been encouraging, with major responses occurring in 5–17% of patients [32,33], suggesting the possibility that chemotherapy is promising as a modality for RCC therapy if anticancer agents can be selectively delivered, released, and maintained around tumor tissues. Compared with CPT-11, NK012 had significant antitumor activity against both bulky Renca (mouse renal cell tumor) and SKRC-49 tumors. Notably, NK012 eradicated rapid-growing Renca tumors in 6 of 10 mice [34]. In the pulmonary metastasis treatment model, an enhanced and prolonged distribution of free SN-38 was observed in metastatic lung tissues but not in non-metastatic lung tissues after NK012 administration. NK012 treatment resulted in a significant decrease in metastatic nodule number and was of survival benefit. Our study showed the outstanding advantage of polymeric micelle-based drug carriers and suggests that NK012 would be effective in treating disseminated RCCs with irregular vascular architectures.

3.4. Glioma

Irinotecan hydrochloride (CPT-11), a prodrug of SN-38, shows some antitumor activities in patients with recurrent gliobastoma multiforme (GBM), with response rates of 0 to 17% in several trials [35–38]. CPT-11 activity is thus similar to that of other agents used for recurrent GBM [37]. A recent phase II trial for recurrent GBM demonstrated that the combination of CPT-11 and bevacizumab, an anti-vascular endothelial growth factor (VEGF) monoclonal antibody, is an effective treatment against the neoplasia with a 6-month progression-free survival rate of 46% and a 6-month overall survival rate of 77% [39,40]. However, there is an increased risk of developing venous thromboembolic disease and intracranial hemorrhage with this combination therapy [40]. Therefore, there is an urgent need to develop treatment modalities by which cytotoxic drugs can exert more potent antitumor activity to their full potential with modest adverse effects and thereby reasonably prolong the overall survival in GBM patients. Our study showed that the therapeutic effect of NK012 was superior to that of CPT-11 in terms of antitumor effect and survival. Since the antitumor activity of SN-38 is time dependent, the superiority of NK012 over CPT-11 may be due to the enhanced accumulation of NK012 and the prolonged sustained

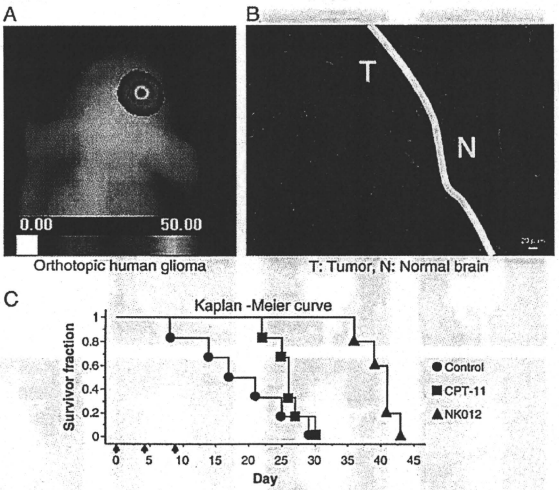

Fig. 4. Antitumor effect of NK012 or CPT-11 on orthotopic xenograft. (A) and survival. 0.9% NaCl solution (●), NK012 (30 mg/kg/day, ▲), or CPT-11 (66.7 mg/kg/day, ■) on days 0 (20 days after tumor inoculation), 4, and 8 (arrows). (B) Distribution of NK012 or CPT-11 in U87MG/Luc glioma xenografts. Tumor tissues were excised 24 h after the intravenous injection of NK012 or CPT-11. Each mouse was administered fluorescein-labeled *Lycopersicon esculentum* lectin 5 min before sacrifice to detect tumor blood vessels. Frozen sections were examined under a fluorescence microscope at an excitation wavelength of 377 nm and an emission wavelength of 477 nm. The same fluorescence conditions can be applied for visualizing NK012 and CPT-11 fluorescence. Free SN-38 could not be detected under these fluorescence conditions. The white lines indicate the border between the tumor and the brain tissue. T, U87MG/Luc tumor; N, normal brain tissue. (Scale bars: 20 μm.). (C) Treatment effects of NK012 on survival. Survival was assessed by Kaplan–Meier analysis. Each group consisted of 6 mice.

release of SN-38 from NK012 within the tumor tissues. Nevertheless, free SN-38 was not detected in the normal brain tissues at any measurement time after intravenous injection of NK012 or CPT-11. It is thus speculated that both NK012 and CPT-11 are unable to cross the blood brain barrier (BBB) in the normal brain, but can pass through the brain tumor vessels effectively [41] (Fig. 4). In addition, CPT-11 in combination with bevacizumab showed significantly more potent antitumor activity and longer survival than CPT-11 monotherapy. However, there was no difference between NK012 monotherapy and NK012 in combination with bevacizumab. Concentration of free SN-38 released from NK012 in the tumor tissue decreased in combination with bevacizumab. NK012 monotherapy or NK012 with bevacizumab showed potent antitumor activity and longer survival than any dosing method of CPT-11 in combination with bevacizumab [42]. Our data warrant a clinical evaluation of NK012 in patients with GBM.

3.5. Stomach cancer

Patients with gastric cancer with scirrhous type stroma particularly demonstrated poor prognosis even after curative resection, as well as highly progressed peritoneal dissemination [43]. Since peritoneal dissemination causes several refractory symptoms such as massive ascites, intestinal obstruction, hydronephrosis and obstructive jaundice, the quality of life of patients at the end stage of cancer is severely impaired. Poor delivery of anticancer drugs to peritoneal metastatic cells may be one of the reasons for the poor prognosis of patients with peritoneal dissemination [44]. In peritoneal nodules, the distribution and eventual diffusion of drugs to cancer cells tend to be impeded because of several obstacles such as severe fibrosis and high interstitial pressure [45,46]. On the other hand, angiogenesis was reported to be an essential factor in the development of peritoneal metastasis, and the

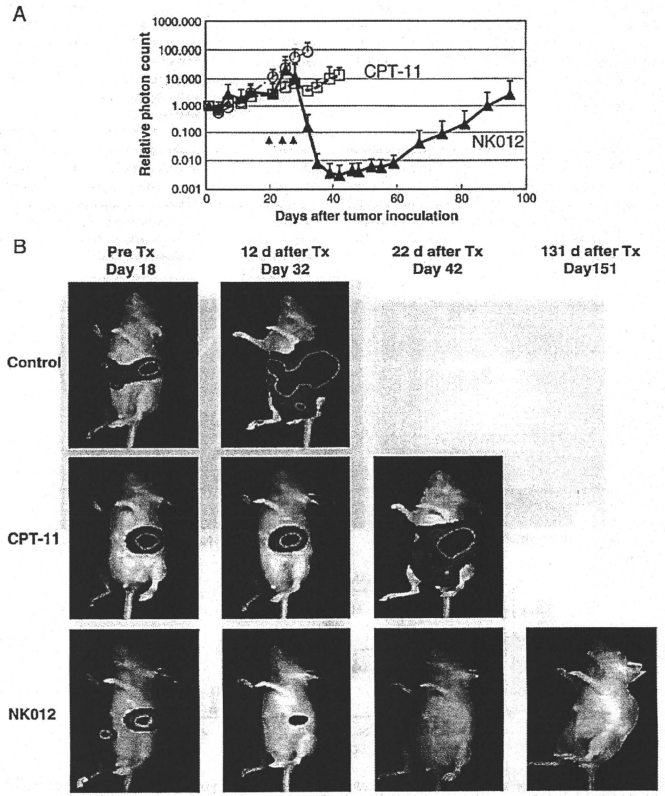

Fig. 5. Effects of NK012 and CPT-11 in 44As3Luc mouse models. Antitumor activity of NK012 or CPT-11 was evaluated by counting the number of photons using the IVIS system (points, mean; bars, SD; arrows, drug injections). A. Antitumor effect of each regimen on days 20, 24 and 28. (○) control, (□) CPT-11 (66.7 mg/kg/day, ×3) and (▲) NK012 (30 mg/kg/day,×3) in 44As3Luc mouse model. B. Images of 44As3Luc mouse model administered NK012 taken using the IVIS system on days 18, 32, 42 and 151 after inoculation of 44As3Luc cells. Data were derived from the same mice as those used in the present study.

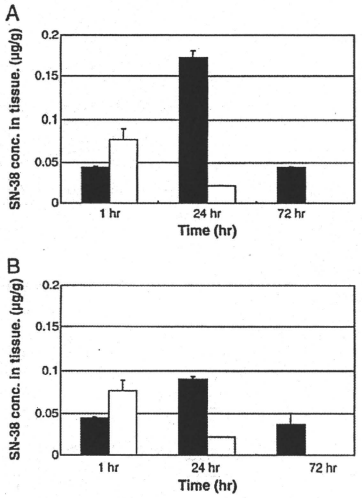

Fig. 6. Concentration-time profile of free SN-38. NK012 (30 mg/kg) or CPT-11 (66.7 mg/kg) was injected 26 days after implantation of 44As3Luc gastric cancer cells (points, mean; bars, SD). A. Concentration of free SN-38 in orthotopic gastric tumor tissue of 44As3Luc mouse model after administration of NK012 (black column) and CPT-11 (white column). B. Concentration of free SN-38 in peritoneal nodules of 44As3Luc mouse model after administration of NK012 (black column) and CPT-11 (white column).

high expression level of vascular endothelial growth factor (VEGF) in primary gastric tumors or ascitic fluid, which can enhance tumor vascular permeability, was found to be directly associated with the development of ascites and peritoneal dissemination [47–51]. In addition, several factors such as kinins and nitric oxide are known to be involved in tumor vascular permeability [52–54]. We evaluated the antitumor activity of NK012 against peritoneal tumor dissemination as compared with that of CPT-11 using mouse models orthotopically transplanted with scirrhous gastric cancer cells, as well as against spontaneously progressing peritoneal dissemination [55,56]. NK012 or CPT-11 distribution in these tumors was evaluated using a fluorescence microscope on the same schedule. In both models, the antitumor activity of NK012 was superior to that of CPT-11 (Fig. 5A and B). High concentration of SN-38 released from NK012 was detected in gastric tumors and peritoneal nodules up to 72 h by HPLC (Fig. 6A and B). Only a slight conversion from CPT-11 to SN-38 was observed from 1 to 24 h. Fluorescence originated from NK012 was detected up to 72 h, whereas that from CPT-11 disappeared until 24 h. NK012 also showed antitumor activity against peritoneal nodules [57]. Thus, NK012 showing enhanced distribution with prolonged SN-38 release may be ideal for cancer treatment especially in patients with stomach cancer.

3.6. Colorectal cancer (CRC)

In two phase III trials, the addition of CPT-11 to bolus or infusional 5-FU-leucovorin (5FU/LV) regimens clearly yielded greater efficacy than administration of 5FU/LV alone, with a doubling of the tumor response rate and prolongation of the median survival time by 2–3 months [1,2]. We evaluated the antitumor activity of NK012 administered in combination with 5FU as compared with that of CPT-11 administered in combination with 5FU against CRC in an experimental model. And we found that the therapeutic effect of NK012/5FU was significantly superior to that of CPT-11/5FU against HT-29 tumors [58].

4. Phase I clinical trials

Two independent phase I clinical trials were conducted in the National Cancer Center in Japan [59] and the Sarah Canon Cancer Center in the USA [60] in patients with advanced solid tumors to define the maximum tolerated dose (MTD), dose limiting toxicity

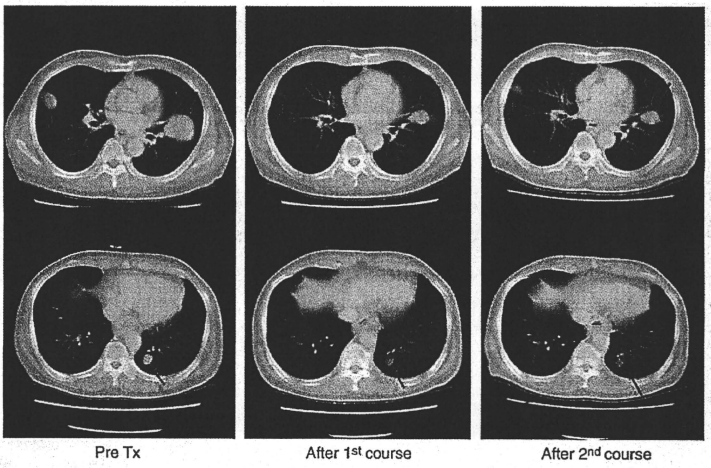

Fig. 7. Computed tomography scan of a patient with conventional-chemotherapy-refractory esophageal cancer with multiple pulmonary metastases showing a reduction in tumor burden after two cycles of NK012 at a dose level of 28 mg/m^2 and continuing study therapy for 5 months until disease progression.

(DLT), and recommended dose for phase II study. NK012 is infused intravenously over 30 min every 21 days until disease progression or unacceptable toxicity occurs. The MTD was 37 mg/m^2 in the US, however 28 mg/m^2 in Japan. The recommended dose (RD) for phase 2 study was the same 28 mg/m^2 in both countries. DLTs were mostly neutropenia or its related events, and diarrhea was mild. The PK profile in the US study was similar to that in the Japanese study. Antitumor activity was also promising. Partial responses (PRs) were obtained in 3 patients with triple negative breast cancer, 1 patient with SCLC, 1 patient with endometrial cancer, and 1 patient with pancreatic neuroendocrine tumor in the USA trial. In Japanese trial, PRs were obtained in 1 patient with esophageal cancer and 1 patient with lung carcinoid (Fig. 7). A phase II study in patients with colorectal cancers is now underway in Japan. In the USA, 2 phase II studies were underway in patients with triple negative breast cancer and patients with SCLC.

5. Conclusion

NK012 is categorized in DDS and the data from several preclinical studies shows that the formulation appears to accumulate selectively and remain for a long time in solid tumor tissues by utilizing the EPR effect.

Our preclinical study showed that the CPT-11-induced mucosal change in mouse intestine was mainly fibrosis considered to be a form of recovery change from erosion. On the other hand, the small intestinal mucosa of the mice in the NK012 treatment group showed only mild shortening and decreased number of villi or mild inflammatory cell invasion. It is too early to conclude that NK012 may cause weaker diarrhea than CPT-11, but the present results within a Phase I setting may encourage further clinical evaluation regarding intestinal toxicity of NK012.

Regarding higher response rate within phase 1 setting, in tumor tissue, we speculate that NK012 accumulates to a greater extent and stays longer in tumor tissue since it is stable in circulation and exhibits markedly higher plasma AUC than CPT-11. Moreover, NK012 appears to induce sustained release of SN-38 inside the tumor following the accumulation of NK012 in the tumor tissue. It is speculated that this pharmacokinetic characteristics of NK012 can produce a higher antitumor activity in clinics.

The favorable safety profile and promising clinical antitumor activity of NK012 warrant further clinical evaluation.

References

[1] L.B. Saltz, J.V. Cox, C. Blanke, L.S. Rosen, L. Fehrenbacher, M.J. Moore, J.A. Maroun, S.P. Ackland, P.K. Locker, N. Pirotta, G.L. Elfring, L.L. Miller, Irinotecan plus fluorouracil and leucovorin for metastatic colorectal cancer Irinotecan Study Group, N Engl J. Med. 343 (2000) 905–914.

[2] J.Y. Douillard, D. Cunningham, A.D. Roth, M. Navarro, R.D. James, P. Karasek, P. Jandik, T. Iveson, J. Carmichael, M. Alakl, G. Gruia, L. Awad, P. Rougier, Irinotecan combined with fluorouracil compared with fluorouracil alone as first-line treatment for metastatic colorectal cancer: a multicentre randomised trial, Lancet 355 (2000) 1041–1047.

[3] D. Cunningham, S. Pyrhönen, R.D. James, C.J. Punt, T.F. Hickish, R. Heikkila, T.B. Johannesen, H. Starkhammar, C.A. Topham, L. Awad, C. Jacques, P. Herait, Randomised trial of irinotecan plus supportive care versus supportive care alone after fluorouracil failure for patients with metastatic colorectal cancer, Lancet 352 (1998) 1413–1418.

[4] K. Noda, Y. Nishiwaki, M. Kawahara, S. Negoro, T. Sugiura, A. Yokoyama, M. Fukuoka, K. Mori, K. Watanabe, T. Tamura, S. Yamamoto, N. Saijo, Irinotecan plus cisplatin compared with etoposide plus cisplatin for extensive small-cell lung cancer, N Engl J. Med. 346 (2002) 85–91.

[5] C.H. Takimoto, S. Arbuck, Topoisomerase I Targeting Agents: the Camptothecines, 3rd edLippencott Willams & Wilkins, 2001.

[6] M.L. Rothenberg, J.G. Kuhn, H.A. Burris III, J. Nelson, John R. Eckardt, M. Tristan-Morales, Susan G. Hilsenbeck, Geoffrey R. Weiss, Lon S. Smith, Gladys I. Rodriguez, Michael K. Rock, Daniel D. Von Hoff, Phase I and pharmacokinetic trial of weekly CPT-11, J. Clin. Oncol. 11 (1993) 2194–2204.

[7] J.G. Slatter, L.J. Schaaf, J.P. Sams, K.L. Feenstra, M.J. Johnson, P.A. Bombardt, K.S. Cathcart, M.T. Verburg, L.K. Pearson, L.D. Compton, L.L. Miller, D.S. Baker, C.V. Pesheck, R.S. Lord III, Pharmacokinetics, metabolism, and excretion of irinotecan (CPT-11) following I.V. infusion of [(14)C]CPT-11 in cancer patients, Drug Metab. Dispos. 28 (2000) 423–433.

[8] S. Guichard, C. Terret, I. Hennebelle, I. Lochon, P. Chevreau, E. Fr_tigny, J. Selves, E. Chatelut, R. Bugat, P. Canal, CPT-11 converting carboxylesterase and topoisomerase activities in tumour and normal colon and liver tissues, Br. J. Cancer 80 (1999) 364–370.

[9] K. Kataoka, G.S. Kwon, M. Yokoyama, T. Okano, Y. Sakurai, Block copolymer micelles as vehicles for drug delivery, J. Control. Release 24 (1993) 119–132.

[10] M. Yokayama, M. Miyauchi, N. Yamada, T. Okano, K. Kataoka, S. Inoue, Polymer micelles as novel drug carrier: adriamycin-conjugted poly(ethylene glycol)–poly (aspartic acid) block copolymer, J. Control. Release 11 (1990) 269–278.

[11] M. Yokoyama, T. Okano, Y. Sakurai, H. Ekimoto, C. Shibazaki, K. Kataoka, Toxicity and antitumor activity against solid tumors of micelle-forming polymeric anticancer drug and its extremely long circulation in blood, Cancer Res. 51 (1991) 3229–3236.

[12] Y. Matsumura, H. Maeda, A new concept for macromolecular therapeutics in cancer chemotherapy: mechanism of tumoritropic accumulation of proteins and the antitumor agent smancs, Cancer Res. 46 (1986) 6387–6392.

[13] F. Koizumi, M. Kitagawa, T. Negishi, T. Onda, S. Matsumoto, T. Hamaguchi, Y. Matsumura, Novel SN-38-incorporating polymeric micelles, NK012, eradicate vascular endothelial growth factor-secreting bulky tumors, Cancer Res. 66 (2006) 10048–10056.

[14] H. Cabral, N. Nishiyama, S. Okazaki, H. Koyama, K. Kataoka, Preparation and biological properties of dichloro(1,2-diaminocyclohexane)platinum(II) (DACHPt)-loaded polymeric micelles, J. Controlled Res 101 (2005) 223–232.

[15] N. Nishiyama, M. Yokoyama, T. Aoyagi, T. Okano, Y. Sakurai, K. Kataoka, Preparation and characterization of self-assembled polymer–metal complex micelle from cis-dichlorodiammineplatinum(II) and poly(ethylene glycol)–poly (α,β-aspartic acid) block copolymer in an aqueous medium, Langmuir 15 (1999) 377–383.

[16] A. Jemal, R. Siegel, E. Ward, Y. Hao, J. Xu, T. Murray, M.J. Thun, Cancer statistics, 2008, CA Cancer J. Clin. 58 (2008) 71–96.

[17] A.L. Warshaw, C.C. Fern_ndez-del, Pancreatic carcinoma, N Engl J. Med. 326 (1992) 455–465.

[18] H.J. Wanebo, M.P. Vezeridis, Pancreatic carcinoma in perspective. A continuing challenge, Cancer 78 (1996) 580–591.

[19] E.S. Casper, M.R. Green, D.P. Kelsen, R.T. Heelan, T.D. Brown, C.D. Flombaum, B. Trochanowski, P.G. Tarassoff, Phase II trial of gemcitabine (2,2'-difluorodeoxycytidine) in patients with adenocarcinoma of the pancreas, Invest. New Drugs 12 (1994) 29–34.

[20] J. Carmichael, U. Fink, R.C. Russell, M.F. Spittle, A.L. Harris, G. Spiessi, J. Blatter, Phase II study of gemcitabine in patients with advanced pancreatic cancer, Br. J. Cancer 73 (1996) 101–105.

[21] M.J. Moore, D. Goldstein, J. Hamm, A. Figer, J.R. Hecht, S. Gallinger, H.J. Au, P. Murawa, D. Walde, R.A. Wolff, D. Campos, R. Lim, K. Ding, G. Clark, T. Voskoglou-Nomikos, M. Ptasynski, W. Parulekar, Erlotinib plus gemcitabine compared with gemcitabine alone in patients with advanced pancreatic cancer: a phase III trial of the National Cancer Institute of Canada Clinical Trials Group, J. Clin. Oncol. 25 (2007) 1960–1966.

[22] T. Hosoki, Dynamic CT of pancreatic tumors, AJR Am. J. Roentgenol. 140 (1983) 959–965.

[23] A. Sofuni, H. Iijima, F. Moriyasu, D. Nakayama, M. Shimizu, K. Nakamura, F. Itokawa, T. Itoi, Differential diagnosis of pancreatic tumors using ultrasound contrast imaging, J. Gastroenterol. 40 (2005) 518–525.

[24] Y. Saito, M. Yasunaga, J. Kuroda, Y. Koga, Y. Matsumura, Antitumour activity of NK012, SN-38-incorporating polymeric micelles, in hypovascular orthotopic pancreatic tumour, Eur. J. Cancer 46 (2010) 650–658.

[25] K. Noda, Y. Nishiwaki, M. Kawahara, S. Negoro, T. Sugiura, A. Yokoyama, M. Fukuoka, K. Mori, K. Watanabe, T. Tamura, S. Yamamoto, N. Saijo, Irinotecan plus cisplatin compared with etoposide plus cisplatin for extensive small-cell lung cancer, N Engl J. Med. 346 (2002) 85–91.

[26] N. Masuda, M. Fukuoka, Y. Kusunoki, K. Matsui, N. Takifuji, S. Kudoh, S. Negoro, M. Nishioka, K. Nakagawa, M. Takada, CPT-11: a new derivative of camptothecin for the treatment of refractory or relapsed small-cell lung cancer, J. Clin. Oncol. 10 (1992) 1225–1229.

[27] R. Atsumi, W. Suzuki, H. Hakusui, Identification of the metabolites of irinotecan, a new derivative of camptothecin, in rat bile and its biliary excretion, Xenobiotica 21 (1991) 1159–1169.

[28] X.Y. Chu, Y. Kato, Y. Sugiyama, Multiplicity of biliary excretion mechanisms for irinotecan, CPT-11, and its metabolites in rats, Cancer Res. 57 (1997) 1934–1938.

[29] K. Takasuna, T. Hagiwara, M. Hirohashi, M. Kato, M. Nomura, E. Nagai, T. Yokoi, T. Kamataki, Involvement of beta-glucuronidase in intestinal microflora in the intestinal toxicity of the antitumor camptothecin derivative irinotecan hydrochloride (CPT-11) in rats, Cancer Res. 56 (1996) 3752–3757.

[30] T. Nagano, M. Yasunaga, K. Goto, H. Kenmotsu, Y. Koga, J. Kuroda, Y. Nishimura, T. Sugino, Y. Nishiwaki, Y. Matsumura, Antitumor activity of NK012 combined with cisplatin against small cell lung cancer and intestinal mucosal changes in tumor-bearing mouse after treatment, Clin. Cancer Res. 15 (13) (2009 Jul 1) 4348–4355.

[31] T. Nagano, M. Yasunaga, K. Goto, H. Kenmotsu, Y. Koga, J. Kuroda, Y. Nishimura, T. Sugino, Y. Nishiwaki, Y. Matsumura, Synergistic Antitumor Activity of the SN-38-Incorporating Polymeric Micelles NK012 with S-1 in a Mouse Model of Non-Small Cell Lung Cancer, Int J Cancer 127 (2010) 2699–2706.

[32] B.I. Rini, N.J. Vogelzang, M.C. Dumas, J.L. Wade III, D.A. Taber, W.M. Stadler, Phase II trial of weekly intravenous gemcitabine with continuous infusion fluorouracil in patients with metastatic renal cell cancer, J. Clin. Oncol. 18 (2000) 2419–2426.

[33] D.M. Nanus, A. Garino, M. Milowsky, M. Larkin, J.P. Dutcher, Active chemotherapy for sarcomatoid and rapidly progressing renal cell carcinoma, Cancer 101 (2004) 1545–1551.

[34] M. Sumitomo, F. Koizumi, T. Asano, A. Horiguchi, K. Ito, T. Asano, T. Kakizoe, M. Hayakawa, Y. Matsumura, Novel SN-38-incorporated polymeric micelle, NK012, strongly suppresses renal cancer progression, Cancer Res. 68 (6) (2008 Mar 15) 1631–1635.
[35] H.S. Friedman, W.P. Petros, A.H. Friedman, L.J. Schaaf, T. Kerby, J. Lawyer, M. Parry, P.J. Houghton, S. Lovell, K. Rasheed, T. Cloughsey, E.S. Stewart, O.M. Colvin, J.M. Provenzale, R.E. McLendon, D.D. Bigner, I. Cokgor, M. Haglund, J. Rich, D. Ashley, J. Malczyn, G.L. Elfring, L.L. Miller, Irinotecan therapy in adults with recurrent or progressive malignant glioma, J. Clin. Oncol. 17 (1999) 1516–1525.
[36] T.F. Cloughesy, E. Filka, J. Kuhn, G. Nelson, F. Kabbinavar, Friedman H, L L. Miller, G. L. Elfring, Two studies evaluating irinotecan treatment for recurrent malignant glioma using an every-3-week regimen, Cancer 97 (2003) 2381–2386.
[37] M.C. Chamberlain, Salvage chemotherapy with CPT-11 for recurrent glioblastoma multiforme, J. Neurooncol. 56 (2002) 183–188.
[38] M.D. Prados, K. Lamborn, W.K. Yung, K. Jaeckle, H. Robins, M. Mehta, H.A. Fine, P.Y. Wen, T. Cloughesy, S. Chang, M.K. Nicholas, D. Schiff, H. Greenberg, L. Junck, K. Fink, K. Hess, J. Kuhn, A phase 2 trial of irinotecan (CPT-11) in patients with recurrent malignant glioma: a North American Brain Tumor Consortium study, Neuro-Oncol. 8 (2006) 189–193.
[39] J.J. Vredenburgh, A. Desjardins, J.E. Herndon II, J.M. Dowell, D.A. Reardon, J.A. Quinn, J.N. Rich, S. Sathornsumetee, S. Gururangan, M. Wagner, D.D. Bigner, A.H. Friedman, H.S. Friedman, Phase II trial of bevacizumab and irinotecan in recurrent malignant glioma, Clin. Cancer Res. 13 (2007) 1253–1259.
[40] J.J. Vredenburgh, A. Desjardins, J.E. Herndon II, J. Marcello, D.A. Reardon, J.A. Quinn, J.N. Rich, S.S. Sathornsumetee, S. Gururangan, J. Sampson, M. Wagner, L. Bailey, D.D. Bigner, A.H. Friedman, H.S. Friedman, Bevacizumab plus irinotecan in recurrent glioblastoma multiforme, J. Clin. Oncol. 25 (2007) 4722–4729.
[41] J. Kuroda, J. Kuratsu, M. Yasunaga, Y. Koga, Y. Saito, Y. Matsumura, Potent antitumor effect of SN-38-incorporating polymeric micelle, NK012, against malignant glioma, Int. J. Cancer 124 (11) (2009 Jun 1) 2505–2511.
[42] J. Kuroda, J. Kuratsu, M.Yasunaga, Y. Koga, H. Kenmotsu, T. Sugino, Y.Matsumura. Antitumor effect of NK012, a 7-ethyl-10-hydroxycamptothecin-incorporating polymeric micelle, on U87MG orthotopic glioblastoma in mice compared with irinotecan hydrochloride in combination with bevacizumab. Clin Cancer Res. Jan 15;16(2):521–529.
[43] Y. Maehara, S. Moriguchi, H. Orita, Y. Kakeji, M. Haraguchi, D. Korenaga, K. Sugimachi, Lower survival rate for patients with carcinoma of the stomach of Borrmann type IV after gastric resection, Surg. Gynecol. Obstet. 175 (1992) 13–16.
[44] Y. Yonemura, Mechanisms of drug resistance in gastric cancer, in: Y. Yonemura (Ed.), Contemporary Approaches Toward Cure of Gastric Cancer, Kanazawa: Maeda Shoten Co. Ltd, 1996, pp. 87–91.
[45] Y. Matsumura, Y.S. Chung, S. Nishimura, T. Inoue, M. Sowa, Fibrosis in the peritoneum induced by scirrhous gastric cancer cells may act as "soil" for peritoneal dissemination, Cancer 77 (1996) 1668–1675.
[46] R.K. Jain, Barriers to drug delivery in solid tumors, Sci. Am. 271 (1994) 58–65.
[47] D.R. Senger, S.J. Galli, A.M. Dvorak, C.A. Perruzzi, V.S. Harvey, H.F. Dvorak, Tumor cells secrete a vascular permeability factor that promotes accumulation of ascites fluid, Science 219 (1983) 983–985.
[48] H.F. Dvorak, L.F. Brown, M. Detmar, A.M. Dvorak, Vascular permeability factor/vascular endothelial growth factor, microvascular hyperpermeability, and angiogenesis, Am. J. Pathol. 146 (1995) 1029–1039.
[49] J.A. Nagy, E.M. Masse, K.T. Herzberg, M.S. Meyers, K.T. Yeo, T.K. Yeo, T.M. Sioussat, H.F. Dvorak, Pathogenesis of ascites tumor growth: vascular permeability factor, vascular hyperpermeability, and ascites fluid accumulation, Cancer Res. 55 (1995) 360–368.
[50] C.A. Boocock, D.S. Charnock-Jones, A.M. Sharkey, J. McLaren, P.J. Barker, K.A. Wright, P.R. Twentyman, S.K. Smith, Expression of vascular endothelial growth factor and its receptors flt and KDR in ovarian carcinoma, J. Natl Cancer Inst. 87 (1995) 506–516.
[51] K. Aoyagi, K. Kouhuji, S. Yano, M. Miyagi, T. Imaizumi, J. Takeda, K. Shirouzu, VEGF significance in peritoneal recurrence from gastric cancer, Gastric Cancer 8 (2005) 155–163.
[52] H. Maeda, Y. Matsumura, H. Kato, Purification and identification of [hydroxyprolyl3]bradykinin in ascitic fluid from a patient with gastric cancer, J. Biol. Chem. 263 (1988) 16051–16054.
[53] Y. Matusmura, K. Maruo, M. Kimura, T. Yamamoto, T. Konno, H. Maeda, Kinin-generating cascade in advanced cancer patients and in vitro study, Jpn J. Cancer Res. 82 (1991) 732–741.
[54] J. Wu, T. Akaike, K. Hayashida, Y. Miyamoto, T. Nakagawa, K. Miyakawa, W. M_ller-Esterl, H. Maeda, Identification of bradykinin receptors in clinical cancer specimens and murine tumor tissues, Int. J. Cancer 98 (2002) 29–35.
[55] K. Yanagihara, M. Takigahira, H. Tanaka, T. Komatsu, H. Fukumoto, F. Koizumi, K. Nishio, T. Ochiya, Y. Ino, S. Hirohashi, Development and biological analysis of peritoneal metastasis mouse models for human scirrhous stomach cancer, Cancer Sci. 96 (2005) 323–332.
[56] K. Yanagihara, M. Takigahira, F. Takeshita, T. Komatsu, K. Nishio, F. Hasegawa, T. Ochiya, A photon counting technique for quantitatively evaluating progression of peritoneal tumor dissemination, Cancer Res. 66 (2006) 7532–7539.
[57] T.E. Nakajima, K. Yanagihara, M. Takigahira, M. Yasunaga, K. Kato, T. Hamaguchi, Y. Yamada, Y. Shimada, K. Mihara, T. Ochiya, Y. Matsumura, Antitumor effect of SN-38-releasing polymeric micelles, NK012, on spontaneous peritoneal metastases from orthotopic gastric cancer in mice compared with irinotecan, Cancer Res. 68 (22) (2008 Nov 15) 9318–9322.
[58] T.E. Nakajima, M. Yasunaga, Y. Kano, F. Koizumi, K. Kato, T. Hamaguchi, Y. Yamada, K. Shirao, Y. Shimada, Y. Matsumura, Synergistic antitumor activity of the novel SN-38-incorporating polymeric micelles, NK012, combined with 5-fluorouracil in a mouse model of colorectal cancer, as compared with that of irinotecan plus 5-fluorouracil, Int. J. Cancer 122 (9) (2008 May 1) 2148–2153.
[59] K. Kato, T. Hamaguchi, K. Shirao, Y. Shimada, T. Doi, A. Ohtsu, Y. Matsumura, Y. Yamada, Interim analysis of phase I study of NK012, polymer micelle SN-38, in patients with advanced cancer, Proc. Am. Soc. Clin. Oncol. (2008) Abs#485.
[60] H.A. Burris III, J.R. Infante, D.R. Spigel, F.A. Greco, D.S. Thompson, S. Matsumoto, S. Kawamura, S.F. Jones, A phase I dose-escalation study of NK012, Proc. Am. Soc. Clin. Oncol. (2008) Abs#2538.

Published OnlineFirst October 13, 2010; DOI:10.1158/1078-0432.CCR-10-0387

Clinical Cancer Research

Phase I Study of NK012, a Novel SN-38–Incorporating Micellar Nanoparticle, in Adult Patients with Solid Tumors

Tetsuya Hamaguchi, Toshihiko Doi, Takako Eguchi-Nakajima, et al.

Clin Cancer Res 2010;16:5058-5066. Published OnlineFirst October 13, 2010.

Published OnlineFirst October 13, 2010; DOI:10.1158/1078-0432.CCR-10-0387

Cancer Therapy: Clinical

Clinical Cancer Research

Phase I Study of NK012, a Novel SN-38–Incorporating Micellar Nanoparticle, in Adult Patients with Solid Tumors

Tetsuya Hamaguchi[1], Toshihiko Doi[4], Takako Eguchi-Nakajima[1], Ken Kato[1], Yasuhide Yamada[1], Yasuhiro Shimada[1], Nozomu Fuse[4], Atsushi Ohtsu[4], Shin-ichi Matsumoto[2], Masaya Takanashi[3], and Yasuhiro Matsumura[5]

Abstract

Purpose: We conducted a first-in-human phase I study to determine the dose-limiting toxicity (DLT), evaluate the pharmacokinetic profile, and document any antitumor activity of NK012, a novel SN-38–incorporating micellar nanoparticle.

Experimental Design: Patients with solid tumors refractory to standard therapy, or for which no standard therapy is available, were enrolled. NK012 was administered as a 30-minute infusion every 3 weeks. The starting dose was 2 mg/m^2 as SN-38 equivalent, and an accelerated titration schedule was used. Pharmacokinetic analysis was conducted in cycles 1 and 2.

Results: Twenty-four patients were enrolled in the study. No *UGT1A1*28* homozygous patients were enrolled. Predominant toxicity was neutropenia. Nonhematologic toxicity, especially diarrhea, was mostly grade 1 or 2 during study treatments. Two of nine patients had DLT during cycle 1 at the 28 mg/m^2 dose level. DLTs were mostly neutropenia or a related event. Polymer-bound SN-38 (NK012) and SN-38 released from NK012 were slowly eliminated from the plasma, with a terminal-phase half-life of approximately 140 and 210 hours, respectively. Systemic exposure to both polymer-bound SN-38 and SN-38 increased in proportion to the dose. A refractory esophageal cancer patient and a lung carcinoid tumor patient had an objective response and continued the study treatment for 5 and 12 months, respectively.

Conclusions: NK012 was well tolerated and showed antitumor activity including partial responses and several occurrences of prolonged stable disease across a variety of advanced refractory cancers. Phase II studies are ongoing. *Clin Cancer Res; 16(20); 5058–66. ©2010 AACR.*

Irinotecan hydrochloride (CPT-11) has proven to be active against colorectal, lung, and ovarian cancers (1–5). CPT-11 is a prodrug that is converted to a biologically active metabolite, 7-ethyl-10-hydroxy-CPT (SN-38), by carboxylesterase (CE) enzymes. SN-38 is an analogue of the plant alkaloid camptothecin, which targets DNA topoisomerase I. Compared with CPT-11, SN-38 exhibits up to 1,000-fold more potent cytotoxic activity against various cancer cells *in vitro* (6). Although CPT-11 is converted to SN-38 in the liver and tumor, the metabolic conversion rate is <10% of the original volume of CPT-11 (7, 8). Moreover, the conversion of CPT-11 to SN-38 depends on the genetic interindividual variability of CE activity (9). Thus, more efficient use of SN-38 might be highly advantageous and quite attractive for cancer treatment.

Drugs categorized under the drug delivery system (DDS) are made primarily by using nanotechnology (10). In the field of oncology, DDS drugs have been produced and evaluated in preclinical or clinical trials, with some already approved for clinical use (11, 12). NK012 categorized in DDS is a micelle-forming macromolecular prodrug prepared by binding SN-38 to the polyglutamate of a block copolymer via an ester bond (Fig. 1). The amphiphilic block copolymers consist of polyethylene glycol and partially SN-38–bound polyglutamate. Polyethylene glycol is hydrophilic and would form the outer shell of the micelle, producing a "stealth" effect that allows NK012 to avoid uptake by the reticuloendothelial system, and SN-38–bound polyglutamate is hydrophobic and would form the inner core of the micelle. The ester bond between glutamic acid and SN-38 is gradually cleaved by hydrolysis under physiologic conditions. In other words, SN-38 can gradually be released from NK012 in a nonenzymatic

Authors' Affiliations: [1]Division of Gastrointestinal Oncology, National Cancer Center Hospital; [2]Pharmaceutical Research Laboratories and [3]Pharmaceutical Development, Nippon Kayaku Co. Ltd., Tokyo, Japan and [4]Division of Gastrointestinal Oncology and [5]Investigative Treatment Division, National Cancer Center Hospital East, Chiba, Japan

Note: Supplementary data for this article are available at Clinical Cancer Research Online (http://clincancerres.aacrjournals.org/).

Presented in part at the 20th European Organization for Research and Treatment of Cancer–National Cancer Institute–AACR symposium on "Molecular Targets and Cancer Therapeutics," October 21-24, 2008, Geneva, Switzerland, and the American Society of Clinical Oncology 2008 Gastrointestinal Cancers Symposium, January 25-27, Orlando, Florida.

Corresponding Author: Tetsuya Hamaguchi, National Cancer Center Hospital, 5-1-1 Tsukiji, Chuo-ku, Tokyo 104-0045, Japan. Phone: 81-3-3542-2511; Fax: 81-3-3547-6173; E-mail: thamaguc@ncc.go.jp.

doi: 10.1158/1078-0432.CCR-10-0387

Published OnlineFirst October 13, 2010; DOI:10.1158/1078-0432.CCR-10-0387

Translational Relevance

NK012 is an SN-38–loaded polymeric micelle constructed in an aqueous milieu via self-assembly of an amphiphilic block copolymer. NK012, which combines enhanced distribution with prolonged sustained release of SN-38 within tumors, may be ideal for treating solid tumors because the antitumor activity of SN-38 is time dependent. This phase I study was conducted to determine the maximum tolerated dose, dose-limiting toxicities, and pharmacokinetics of NK012 administered as an i.v. infusion every 3 weeks. Two patients achieved partial response, indicating preliminary evidence of antitumor activity. Hematologic toxicities were manageable, and notably, none of the patients experienced grade 3 diarrhea during any cycle. In the pharmacokinetic study, polymer-bound SN-38 (NK012) clearance was significantly lower and released SN-38 concentration in the plasma was maintained for a long time compared with those of conventional CPT-11 at a dose of 250 mg/m^2. Moreover, systemic exposure to both polymer-bound SN-38 and SN-38 increased in proportion to the dose. NK012 warrants further evaluation to assess its efficacy, alone or in combination with other agents, in tumors showing sensitivity to CPT-11.

manner. Therefore, unlike CPT-11, NK012 is expected to exhibit stable drug efficacy regardless of differences in CE activity among patients. NK012 has a diameter of ~20 nm. In preclinical experimental tumor models such as lung cancer (13, 14), pancreatic cancer (15), renal cancer (16), glioma (17), gastric cancer (18), and colorectal cancer (19), NK012 exerted significantly superior antitumor activity and induced longer survival compared with CPT-11. In preclinical pharmacokinetic (PK) studies (13–18), CPT-11 and SN-38 converted from CPT-11 rapidly disappeared from the plasma. On the other hand, polymer-bound SN-38 (NK012) exhibited a lower clearance rate. In the tumor tissues, polymer-bound SN-38 and released SN-38 concentration were also maintained for a long time following injection. Thus, NK012, which combines enhanced distribution with sustained release of SN-38 within tumors, may be ideal for the treatment of solid tumors because the antitumor activity of SN-38 is time dependent (15).

The primary endpoints of this study were to determine the maximum tolerated dose (MTD) and recommended phase II dose of NK012 administered as an i.v. infusion every 3 weeks, evaluate the toxicity profile and PK, and identify any dose-limiting toxicity (DLT). Evidence of antitumor activity was also evaluated.

Materials and Methods

This trial was a two-center (National Cancer Center Hospital, Tokyo and National Cancer Center Hospital East, Chiba), first-in-human, open-label, phase I, dose-escalation study of NK012 in patients with advanced tumors, sponsored by Nippon Kayaku Co. Ltd. (Tokyo, Japan). This study was conducted in accordance with the International Conference on Harmonization Guidelines for Good Clinical Practice and the Declaration of Helsinki.

Patients

Eligible patients had histologically or cytologically confirmed malignant tumors for which standard curative or palliative measures did not exist. Further requirements were as follows: age ≥20 and <75 years; Eastern Cooperative Oncology Group (ECOG) performance status ≤2; life expectancy ≥2 months; and adequate bone marrow, hepatic, renal, and pulmonary function within 1 week before commencing treatment [absolute neutrophil count ≥2,000/μL, platelet count ≥100,000/μL, hemoglobin ≥9 g/dL, total bilirubin ≤1.5 mg/dL, aspartate aminotransferase (AST) and alanine aminotransferase (ALT) ≤2.5 times the upper limit of normal, creatinine ≤1.5 mg/dL, PaO_2 ≥60 mmHg]. Treatment with radiotherapy, endocrine therapy, or chemotherapy must have ceased at least 4 weeks before commencing treatment. Patients with severe, clinically significant, and/or uncontrolled medical conditions were excluded. Patients who had previously been treated with CPT-11 were accepted for enrollment. Our institutional review board granted approval for the study, and written informed consent from each patient was obtained.

Treatment plan

NK012 was supplied by Nippon Kayaku Co. Ltd. The drug was a sterile lyophilized powder and was diluted with 5% glucose for a total volume of 250 mL. This solution was administered by i.v. infusion for 30 minutes every 21 days. This schedule was set based on the nadir point and the period for recovery after the dosing of NK012 according to data from the preclinical study.

No prophylactic agents for emesis or cholinergic reaction were administered. Patients received up to four cycles of NK012, except in the case of unacceptable toxicity, withdrawal of consent, or disease progression. Patients could continue treatment beyond four cycles if the investigator determined that additional treatment would be of further benefit to the patient, as long as toxicity remained acceptable.

Patients were screened for *UGT1A1* polymorphism (*UGT1A1*28* and *UGT1A1*6*) before enrollment. Based on the screening results, patients were separated into two groups: (group 1) patients with wild-type (*wt/wt*), those with *UGT1A1*28* heterozygous genotype (*wt/*28*), or those with *UGT1A1*6* genotype (*wt/*6*, **6/*6*, or **28/*6*), and (group 2) those with *UGT1A1*28* homozygous genotype (**28/*28*). Patients of group 1 received a starting dosage of NK012 of 2 mg/m^2, which is one third the toxic dose low in dogs. As a safety measure, patients of group 2 were treated at a lower dose (confirmed tolerable dose in group 1) to avoid any anticipated severe toxicity in this trial.

Published OnlineFirst October 13, 2010; DOI:10.1158/1078-0432.CCR-10-0387

Assessments, follow-up, and monitoring

Toxic events were observed until resolution to baseline or less than grade 1. Before entry into the study, patients underwent a clinical history and physical examination, performance status assessment, complete blood count, chemistries, urinalysis, pregnancy test (if applicable), chest X-ray, electrocardiogram including assessment of QTc interval, and disease assessment by computed tomography (CT) scan. During therapy, patients were assessed at least weekly for adverse events (AE). CT scanning of disease sites was repeated every two cycles. AEs were classified/graded according to the National Cancer Institute Common Terminology Criteria of Adverse Events (version 3). Response was evaluated in accordance with the Response Evaluation Criteria in Solid Tumors.

DLT was defined as any drug-related grade 4 hematologic toxicity (grade 4 neutropenia ≥5 days, grade 4 thrombocytopenia) and other toxicity grade ≥3 with the exception of nausea, vomiting, loss of appetite, or hypersensitivity. We conducted this dose finding study according to the accelerated titration method described by Simon et al. (20). Namely, because many patients in phase I clinical trials are treated at doses of chemotherapeutic agents that are below the biologically active doses, they have a reduced chance of receiving therapeutic benefit. Therefore, we decided to adopt an accelerated titration followed by a

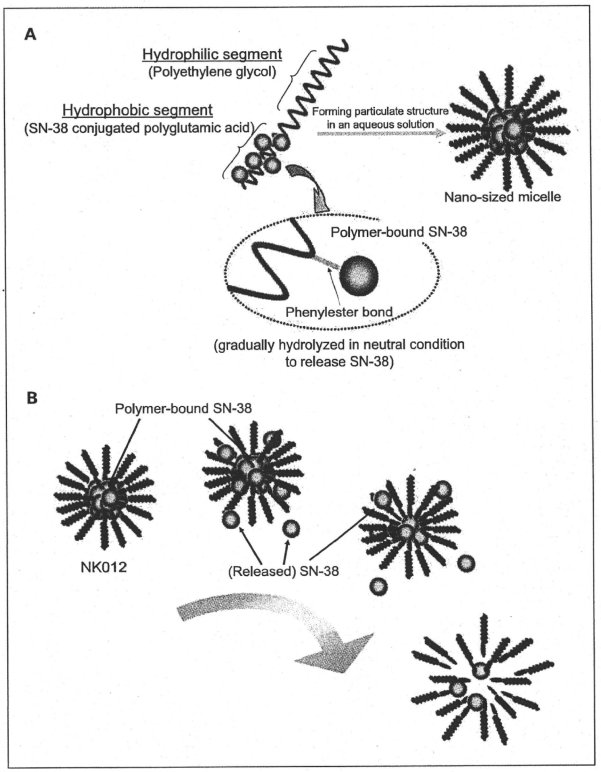

Fig. 1. A, schematic structure of NK012. B, release of SN-38 from NK012.

Published OnlineFirst October 13, 2010; DOI:10.1158/1078-0432.CCR-10-0387

modified Fibonacci method to reduce the number of such patients as described previously (21). In this two-stage design, the first stage allows for a single patient to be enrolled at each dose level. The dose of NK012 is doubled in each successive patient until grade 2 toxicity is observed. If grade 2 toxicity occurs in one patient, that dose level is given to another two patients. This marks the start of the second stage of the design, which is a modified Fibonacci method.

The recommended phase II dose was defined by the Efficacy and Safety Assessment Committee based on the results of this trial. Determination of the MTD/recommended dose was based on the patients of group 1.

PK analysis

Blood samples for PK analysis were obtained on days 1, 2, 3, 4, 8, 15, and 22 of cycle 1 and on days 1 and 2 of cycle 2. Urine samples were collected and pooled over before dosing and 0 to 24 and 24 to 48 hours after the start of infusion in cycle 1. Blood samples were immediately centrifuged, and then a portion of the obtained plasma sample was mixed with an equivalent volume of ice-cold 0.1 mol/L HCl to prevent hydrolysis of NK012. Plasma and urine samples were stored at −80°C until analysis.

The concentration of total SN-38 (the sum of polymer-bound SN-38 and released SN-38), SN-38, and its glucuronide (SN-38G) in the plasma and that of total SN-38 and SN-38G in the urine were assayed by modified reversed-phase high-performance liquid chromatography (HPLC) using fluorescence detection (13). Polymer-bound SN-38 was not quantitated in the urine, as NK012 is unstable in urine. For the respective analytes, proteins were precipitated with an ice-cold mixture of methanol/H_2O/$HClO_4$ (10:9:1, v/v/v). The sample was vortexed for 10 seconds, filtered through a MultiScreen Solvinert (Millipore Corp.), and analyzed. We had previously confirmed that the filtered solution did not contain polymer-bound SN-38. Total SN-38 was determined after alkali hydrolysis. For the plasma matrix, the values for the lower limit of quantitation for total SN-38, SN-38, and SN-38G were 1.0, 0.1, and 0.5 ng/mL, respectively. For the urine, the value for the lower limit of quantitation for both total SN-38 and SN-38G was 10 ng/mL. Polymer-bound SN-38 was determined by subtracting the SN-38 from the total SN-38.

The PK parameters [observed peak plasma concentration (C_{max}), time to peak plasma concentration (T_{max}), half-life of the terminal phase ($t_{1/2z}$), area under the concentration-time curve ($AUC_{inf.}$), total clearance (CL_{tot}), volume of distribution at steady state (V_{ss}), and the mean residence time ($MRT_{inf.}$)] were calculated for each patient using the noncompartmental analysis module of the software program WinNonlin Professional (Pharsight Corp.).

Results

Patient characteristics

Between February 2006 and February 2008, 24 patients with advanced solid tumors were enrolled in the study (Table 1). All the patients except one lung carcinoid patient had received chemotherapy before enrollment. Prior therapies ranged from 1 to 11 regimens of chemotherapy. Fifteen patients, especially all colorectal patients, had previously received CPT-11–based chemotherapy. All the patients were included in the safety analyses. A total of 108 cycles of the study drug was delivered (median, 3.5 cycles; range, 1-12 cycles). Twenty-two patients received more than two administrations. The maximum number of treatments was 12 cycles at 28 mg/m^2. No patients were *UGT1A1*28* homozygous.

Table 1. Patient characteristics

No. patients	24
Sex	
Male	18
Female	6
Age (y)	
Median	61.5
Range	41-74
ECOG performance status	
0	15
1	9
Primary tumor site	
Colorectal	12
Pancreas	4
Small cell lung cancer	3
Esophageal	3
Lung carcinoid	1
Non–small cell lung cancer	1
Prior treatment	
Chemotherapy regimens	
Median	2
Range	0-11
UGT1A1 genotype	
wt/wt	10
*wt/*28*	3
*wt/*6*	10
**6/*28*	1
**6/*6 or *28/*28*	0

Dose-escalation process

Dosage escalation started at 2 mg/m^2 and was gradually increased up to 28 mg/m^2 (Table 2). Clinically meaningful grade 2 NK012-related toxicity was not observed up until 8 mg/m^2 during cycle 1. However, the Efficacy and Safety Assessment Committee recommended raising the dosage by 50% instead of 100% at 12 mg/m^2 and that a modified Fibonacci escalation method should be implemented because the neutrophil count had decreased by 50% compared with the baseline. Therefore, we restarted the dose identification study using a modified Fibonacci method. At a dose level of 20 mg/m^2, one patient experienced grade 4 neutropenia lasting for <5 days. As a safety measure, it was decided that the dose of later cohorts would be increased in increments of 4 mg/m^2, although this AE was

Published OnlineFirst October 13, 2010; DOI:10.1158/1078-0432.CCR-10-0387

not considered DLT. Although 9 of 15 patients at a dose level of 20 to 28 mg/m^2 had either a delay or a reduction in treatment as a result of toxicity (especially neutropenia), only 3 of these patients required dose reduction after DLT; even in the 28 mg/m^2 cohort, 6 of 8 patients successfully continued treatment with NK012 without dose reduction.

Toxicity

NK012 was generally well tolerated. All patients reported AEs considered to be related to NK012, most of which were asymptomatic and grade 1 to 2 in severity: nausea, anorexia, vomiting, fatigue, elevated AST/ALT, elevated γ-glutamyl transpeptidase (γ-GTP), and thrombocytopenia. Three infusion-related reactions were observed at a dose level of 2, 12, and 24 mg/m^2. No cholinergic reactions were observed; such reactions sometimes occur during CPT-11 administration. Fifteen patients reported 36 grade 3 to 4 drug-related AEs (Table 3). The most common grade 3 to 4 events were leukopenia and neutropenia. The median time to the neutrophil nadir at a dose level of 28 mg/m^2 was 12 days (range, 9-21 days), with recovery to grade 1 within 4 to 16 days in cycle 1. No grade 3 or 4 diarrhea was observed.

Four patients reported five serious AEs, three of which were deemed possibly related to NK012: grade 3 infection with neutropenia, grade 4 neutropenia, and grade 3 atrial flutter.

Two of the nine patients treated at a dose level of 28 mg/m^2 experienced DLT during cycle 1. In another independent phase I study of NK012 in the United States, only one of six patients experienced DLT at 28 mg/m^2 during cycle 1, but two of five patients experienced DLT at 37 mg/m^2 during cycle 1 (22). Although the protocol definition of MTD had not been reached, the Efficacy and Safety Assessment Committee recommended discontinuing dose escalation according to the hematologic toxicity profile of our study and another independent phase I study (22). The recommended phase II dose was determined to be 28 mg/m^2 with at least a 3-week interval between treatment cycles.

Table 2. Dose-escalation schema and DLT

NK012 dose (mg/m^2)	Total	DLT			
		Cycle 1	Cycle 2	Cycle 3	Cycle 4
2	1	0	0	0	0
4	1	0	0	0	0
8	1	0	0	0	0
12	3	0	0	0	0
16	3	0	0	0	1*
20	3	0	0	0	0
24	3	0	0	1†	0
28‡	9	2†	1†	1†	1§

*γ-GTP increased.
†Neutropenia or a related event.
‡Recommended dose for phase II studies.
§Atrial flutter.

Efficacy

Twenty-three patients were assessable for response. Two patients had confirmed partial response at a dose of 28 mg/m^2. The first patient, who received CDDP + 5-fluorouracil combination chemotherapy followed by docetaxel monotherapy and had a previously progressing esophageal cancer, achieved a partial response confirmed by CT and continued this therapy for 5 months (serial CT scans can be seen in Supplementary Data). The second patient had a recurrence of lung carcinoid tumor. He developed multiple liver and bone metastases and enrolled in this phase I study because there is no standard systemic chemotherapy for his disease. After four cycles, a partial response was documented. He continued to receive this chemotherapy for 12 months until disease progression. Nine patients had stable disease. In 12 colorectal cancer patients, who were refractory to CPT-11 and oxaliplatin, 5 patients had stable diseases, 4 of whom successfully received six cycles of treatment or more.

Pharmacokinetics

The mean plasma concentration-time profile of polymer-bound SN-38, SN-38, and SN-38G at a dose of 28 mg/m^2 (recommended phase II dose) is shown in Fig. 2A. The concentrations of these analytes in the plasma were maintained over an extended period of time, indicating that NK012 achieved prolonged exposure. There was a proportional increase in C_{max} and $AUC_{inf.}$ values with dose (Fig. 2B and C). The PK parameters are summarized in Table 4. The $t_{1/2z}$ of bound SN-38 was 36.0 to 168 hours, CL_{tot} was 98.8 to 150 mL/h/m^2, V_{ss} was 2,020 to 4,050 mL/m^2, and $MRT_{inf.}$ was 15.9 to 28.6 hours. No significant differences in these parameters were seen in the dose range from 2 to 28 mg/m^2. The $t_{1/2z}$ of SN-38 ranged from 70.7 to 266 hours, and $MRT_{inf.}$ ranged from 47.3 to 109 hours. These parameters were dose independent. Therefore, PK of NK012 proved to be linear in the dose range of 2 to 28 mg/m^2. There was no obvious difference between the plasma concentration of the respective analytes in cycles 1 and 2 (data not shown), although the study design could not fully evaluate the cycle dependency of NK012 PK. The cumulative urinary excretion rate (0-48 hours) of total SN-38 and SN-38G at a dose level of 28 mg/m^2 was 7.0% and 6.8%, respectively. These rates were independent of the dose escalation.

Discussion

In this phase I study, NK012 was well tolerated at doses <28 mg/m^2 every 3 weeks.

Observed toxicity was consistent with CPT-11, a prodrug of SN-38. DLT associated with NK012 was mainly neutropenia. Therefore, it is necessary to pay attention to neutrophil count changes after treatment with NK012; patients with a decreased count should be carefully monitored to prevent infection. Infusion-related reactions characterized by flushing, chest discomfort, or itching occur sometimes during the administration of liposomal

Published OnlineFirst October 13, 2010; DOI:10.1158/1078-0432.CCR-10-0387

Table 3. Highest hematologic and nonhematologic toxicity per patient

A. Hematologic toxicity

Dose (mg/m^2)	*n*	Leukopenia				Neutropenia				Thrombocytopenia			
		Grade				Grade				Grade			
		1	2	3	4	1	2	3	4	1	2	3	4
2	1	0	0	0	0	0	0	0	0	0	0	0	0
4	1	0	0	0	0	0	0	0	0	0	0	0	0
8	1	0	0	0	0	0	0	0	0	0	0	0	0
12	3	0	1	1	0	1	0	1	0	1	0	1	0
16	3	1	2	0	0	2	0	1	0	1	0	0	0
20	3	1	0	2	0	1	0	0	2	0	1	0	0
24	3	0	2	1	0	0	0	2	1	3	0	0	0
28	9	0	1	5	3	0	0	4	5	3	3	0	0
Total	24	2	6	9	3	4	0	8	8	8	4	1	0

B. Nonhematologic toxicity

	2-20 mg/m^2 (*n* = 12)				24 mg/m^2 (*n* = 3)				28 mg/m^2 (*n* = 9)			
	Grade				Grade				Grade			
	1	2	3	4	1	2	3	4	1	2	3	4
Nausea	8	2	0	0	3	0	0	0	3	3	1	0
Anorexia	6	3	0	0	3	0	0	0	3	2	2	0
Diarrhea	3	0	0	0	0	1	0	0	4	4	0	0
Vomiting	3	1	0	0	0	0	0	0	2	3	0	0
Fatigue	7	0	0	0	2	1	0	0	4	2	0	0
Febrile neutropenia	0	0	0	0	0	0	0	0	0	0	1	0
Infection	0	1	0	0	0	0	0	0	0	0	1	0
Atrial flutter	0	0	0	0	0	0	0	0	0	0	1	0
Alopecia	7	1	—	—	1	2	—	—	5	3	—	—
γ-GTP	0	1	1	0	1	0	0	0	2	1	0	0
Rash	2	1	0	0	1	1	0	0	1	2	0	0

and antibody drugs. In this study, only three infusion-related reactions were observed at dose levels of 2, 12, and 24 mg/m^2. However, these infusion reactions were grade 1 and deemed non–dose dependent. The factors associated with the infusion-related reactions remain to be explained. Diarrhea, which is known as a DLT of CPT-11, was mild and transient in this study. Fatigue, nausea, and anorexia were also commonly experienced AEs but were mild and transient. Our preclinical study showed that the CPT-11–induced intestinal mucosal change in mice was active inflammation with cellular invasion, deformed glandular alignment, and glandular duct disappearance. On the other hand, the intestinal mucosa in mice in the NK012 treatment group was almost the same as that in the saline treatment group (14). CPT-11, SN-38, and SN-38G are excreted into the bile and eventually reach the small intestinal lumen (23, 24). SN-38G is deconjugated in the cecum and colon to regenerate SN-38 through bacterial β-glucuronidase (25). Because the CPT-11 dose in the preclinical study was 3-fold higher than that of NK012 at the SN-38 equivalent dose, a higher amount of CPT-11 was found in the intestinal lumen. It is speculated that the highly excreted CPT-11 was reabsorbed in the small intestinal epithelium and converted to SN-38, causing damage to the intestinal mucosa (14). It is too early to conclude that NK012 may cause weaker diarrhea than CPT-11, but the present results within a phase I setting may encourage further clinical evaluation about intestinal toxicity of NK012.

The PK analysis of NK012 suggested that the tissue distribution of SN-38–incorporating micelles is limited. This is consistent with the data obtained in our preclinical study (13). In a phase I study of CPT-11 at doses of 100 to 750 mg/m^2, it was reported that the CL_{tot} and V_{ss} of CPT-11 were 15,000 mL/h/m^2 and 157,000 mL/m^2, respectively (26). Therefore, the present study revealed that the CL_{tot} and V_{ss} of polymer-bound SN-38 were, respectively, approximately 150- and 80-fold lower than those of CPT-11. This suggests that NK012 may have a low distribution in normal tissue after administration. On the other hand, in tumor tissue, we speculate that NK012 accumulates to a greater extent and stays longer in tumor tissue due to the enhanced permeability and retention effect

Published OnlineFirst October 13, 2010; DOI:10.1158/1078-0432.CCR-10-0387

(27) because it is stable in circulation and exhibits a markedly higher plasma AUC than CPT-11. Moreover, NK012 seems to induce sustained release of SN-38 inside the tumor following the accumulation of NK012 in the tumor tissue (13–18).

Sustained exposure to SN-38 is required for successful CPT-11–based chemotherapy because SN-38 induced single-strand DNA breaks in the presence of topoisomerase I and is only effective during the relatively short S phase of the cell cycle (28). When compared with SN-38 converted from conventional CPT-11 at a dose of 250 mg/m^2 (29), SN-38 released from NK012 at 28 mg/m^2 exhibited 2.4-fold greater systemic exposure (0.876 versus 2.12 μg·h/mL) and 15-fold slower elimination from plasma (13.9 versus 209 hours). This result was compatible

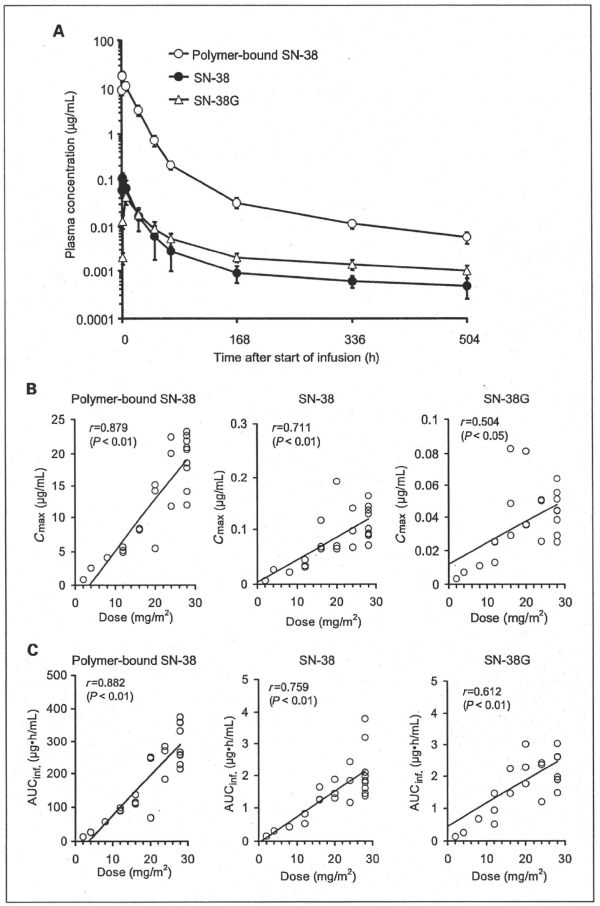

Fig. 2. A, plasma concentration-time profile of polymer-bound SN-38, SN-38, and SN-38G in nine patients after an infusion of NK012 at 28 mg/m^2 in cycle 1. Points, mean; bars, SD. Relationship between dose and C_{max} (B) and between dose and AUC_{inf} (C) of respective analytes in 23 or 24 patients after an infusion of NK012 in cycle 1.

Published OnlineFirst October 13, 2010; DOI:10.1158/1078-0432.CCR-10-0387

Table 4. Plasma PK parameters of (A) polymer-bound SN-38, (B) SN-38, and (C) SN-38G in cycle 1

Dose (mg/m^2)	No. patients	Mean (SD)						
		C_{max} (μg/mL)	T_{max} (h)	$t_{1/2z}$ (h)	$AUC_{inf.}$ (μg·h/mL)	$MRT_{inf.}$ (h)	CL_{tot} ($mL/h/m^2$)	V_{ss} (mL/m^2)
A. Polymer-bound SN-38								
2	1	0.91	1	128	14.1	28.6	142	4,050
4	1	2.60	0.6	36.0	27.0	15.9	148	2,370
8	1	4.16	0.5	102	57.8	19.1	138	2,640
12	3	5.32 (0.38)	0.7 (0.3)	135 (8)	92.4 (5.5)	25.3 (4.0)	130 (7)	3,270 (330)
16	3	8.32 (0.11)	0.8 (0.3)	168 (41)	120 (15)	28.2 (4.0)	134 (15)	3,830 (940)
20	3	11.6 (5.3)	0.8 (0.3)	128 (28)	189 (104)	24.3 (2.0)	150 (121)	3,730 (3,190)
24	3	18.1 (5.6)	0.7 (0.3)	128 (13)	246 (55)	24.5 (0.9)	101 (26)	2,480 (600)
28	9	19.1 (3.9)	0.7 (0.3)	137 (19)	294 (62)	22.2 (2.3)	98.8 (20.6)	2,020 (530)
B. SN-38								
2	1	0.01	1	70.7	0.16	47.3	N/A	N/A
4	1	0.03	0.6	179	0.32	99.9	N/A	N/A
8	1	0.02	1	107	0.430	54.5	N/A	N/A
12	3	0.0377 (0.0073)	0.8 (0.3)	193*	0.683*	70.6*	N/A	N/A
16	3	0.0841 (0.0285)	0.8 (0.3)	250 (60)	1.38 (0.23)	91.4 (23.7)	N/A	N/A
20	3	0.110 (0.072)	0.7 (0.3)	266 (40)	1.55 (0.30)	104 (19)	N/A	N/A
24	3	0.102 (0.036)	0.7 (0.3)	216 (24)	1.81 (0.64)	109 (20)	N/A	N/A
28	9	0.114 (0.031)	0.8 (0.3)	209 (25)	2.12 (0.83)	95.7 (16.7)	N/A	N/A
C. SN-38G								
2	1	0	6	42.7	0.15	50.9	N/A	N/A
4	1	0.01	6	30.8	0.27	38.3	N/A	N/A
8	1	0.01	6	72.9	0.68	75.1	N/A	N/A
12	3	0.02 (0.0071)	6 (0)	171 (102)	0.97 (0.471)	148 (92)	N/A	N/A
16	3	0.05 (0.0272)	6 (0)	294 (61)	2.62 (1.39)	221 (80)	N/A	N/A
20	3	0.05 (0.0266)	6 (0)	264 (70)	2.36 (0.63)	212 (49)	N/A	N/A
24	3	0.0420 (0.0143)	6 (0)	222 (18)	2.00 (0.68)	193 (11)	N/A	N/A
28	9	0.04 (0.0132)	6 (0)	205 (20)	2.28 (0.57)	186 (27)	N/A	N/A

NOTE: Values are represented as the mean (SD).

Abbreviation: N/A, not available.

*n = 2. One patient at 12 mg/m^2 was excluded from the analysis due to the presence of an interference peak on the HPLC chromatogram.

with those obtained in preclinical studies (13, 14, 17). Therefore, the longer systemic exposure time of SN-38 achieved with NK012 therapy is also expected to improve therapeutic efficacy.

Overall, our data suggest that polymer-bound SN-38 and released SN-38 exhibit a linear PK in the dose range of 2 to 28 mg/m^2. In several phase I studies of CPT-11, it was reported that the C_{max} and/or the AUC of CPT-11 increased linearly with the dosage, but the AUC of SN-38 was not as dose dependent as that of CPT-11 or it has no correlation with the dose due to considerable interpatient variability (29–32). Several metabolizing enzymes (e.g., CEs, UGT1A, and CYP3A4) are involved in the disposition of CPT-11 (8, 9, 33). NK012, unlike CPT-11, is hydrolyzed nonenzymatically to release SN-38, resulting in a dose-proportional increase in systemic exposure. Thus, NK012 proved to function steadily as a drug carrier in a dose-independent manner and to release SN-38 in a dose-dependent manner in this phase I trial. In the independent phase I trial conducted in the United States, the PK profile and toxic profile including diarrhea were similar to those of our study. The DLT of the U.S. study was neutropenia and pneumonia with neutropenia. The MTD in the U.S. trial was also determined to be 28 mg/m^2 (22).

In conclusion, the recommended phase II dose of NK012 is 28 mg/m^2 with at least a 3-week interval between treatment cycles. The favorable safety profile and promising clinical antitumor activity warrant further clinical evaluation.

Published OnlineFirst October 13, 2010; DOI:10.1158/1078-0432.CCR-10-0387

Disclosure of Potential Conflicts of Interest

T. Hamaguchi: research grant, Nippon Kayaku Co. Ltd.

Acknowledgments

We thank the patients who participated in this trial, Dr. Toshiharu Yamaguchi for serving as medical consultant, and Kaoru Shiina and Hiromi Orita for their secretarial assistance.

Grant Support

Nippon Kayaku Co. Ltd.
The costs of publication of this article were defrayed in part by the payment of page charges. This article must therefore be hereby marked *advertisement* in accordance with 18 U.S.C. Section 1734 solely to indicate this fact.

Received 02/15/2010; revised 08/05/2010; accepted 08/25/2010; published OnlineFirst 10/12/2010.

References

1. Bodurka DC, Levenback C, Wolf JK, et al. Phase II trial of irinotecan in patients with metastatic epithelial ovarian cancer or peritoneal cancer. J Clin Oncol 2003;21:291–7.
2. Douillard JY, Cunningham D, Roth AD, et al. Irinotecan combined with fluorouracil compared with fluorouracil alone as first-line treatment for metastatic colorectal cancer: a multicentre randomised trial. Lancet 2000;355:1041–7.
3. Negoro S, Masuda N, Takada Y, et al. Randomised phase III trial of irinotecan combined with cisplatin for advanced non-small-cell lung cancer. Br J Cancer 2003;88:335–41.
4. Noda K, Nishiwaki Y, Kawahara M, et al. Irinotecan plus cisplatin compared with etoposide plus cisplatin for extensive small-cell lung cancer. N Engl J Med 2002;346:85–91.
5. Saltz LB, Cox JV, Blanke C, et al, Irinotecan Study Group. Irinotecan plus fluorouracil and leucovorin for metastatic colorectal cancer. N Engl J Med 2000;343:905–14.
6. Takimoto CH, Arbuck S. Topoisomerase I targeting agents: the camptothecines. In: Chabner BA, Lango DL, editors. Cancer Chemotherapy and Biotherapy: Principles and Practice. 3rd edition, Philadelphia: Lippincott Willams & Wilkins; 2001. p. 579–646.
7. Rothenberg ML, Kuhn JG, Burris HA III, et al. Phase I and pharmacokinetic trial of weekly CPT-11. J Clin Oncol 1993;11:2194–204.
8. Slatter JG, Schaaf LJ, Sams JP, et al. Pharmacokinetics, metabolism, and excretion of irinotecan (CPT-11) following I.V. infusion of [(14)C] CPT-11 in cancer patients. Drug Metab Dispos 2000;28:423–33.
9. Guichard S, Terret C, Hennebelle I, et al. CPT-11 converting carboxylesterase and topoisomerase activities in tumour and normal colon and liver tissues. Br J Cancer 1999;80:364–70.
10. Matsumura Y, Kataoka K. Preclinical and clinical studies of anticancer agent-incorporating polymer micelles. Cancer Sci 2009;100:572–9.
11. Gordon AN, Fleagle JT, Guthrie D, Parkin DE, Gore ME, Lacave AJ. Recurrent epithelial ovarian carcinoma: a randomized phase III study of pegylated liposomal doxorubicin versus topotecan. J Clin Oncol 2001;19:3312–22.
12. Gradishar WJ, Tjulandin S, Davidson N, et al. Phase III trial of nanoparticle albumin-bound paclitaxel compared with polyethylated castor oil-based paclitaxel in women with breast cancer. J Clin Oncol 2005;23:7794–803.
13. Koizumi F, Kitagawa M, Negishi T, et al. Novel SN-38-incorporating polymeric micelles, NK012, eradicate vascular endothelial growth factor-secreting bulky tumors. Cancer Res 2006;66:10048–56.
14. Nagano T, Yasunaga M, Goto K, et al. Antitumor activity of NK012 combined with cisplatin against small cell lung cancer and intestinal mucosal changes in tumor-bearing mouse after treatment. Clin Cancer Res 2009;15:4348–55.
15. Saito Y, Yasunaga M, Kuroda J, Koga Y, Matsumura Y. Enhanced distribution of NK012, a polymeric micelle-encapsulated SN-38, and sustained release of SN-38 within tumors can beat a hypovascular tumor. Cancer Sci 2008;99:1258–64.
16. Sumitomo M, Koizumi F, Asano T, et al. Novel SN-38-incorporated polymeric micelle, NK012, strongly suppresses renal cancer progression. Cancer Res 2008;68:1631–5.
17. Kuroda J, Kuratsu J, Yasunaga M, Koga Y, Saito Y, Matsumura Y. Potent antitumor effect of SN-38-incorporating polymeric micelle, NK012, against malignant glioma. Int J Cancer 2009;124:2505–11.
18. Nakajima TE, Yanagihara K, Takigahira M, et al. Antitumor effect of SN-38-releasing polymeric micelles, NK012, on spontaneous peritoneal metastases from orthotopic gastric cancer in mice compared with irinotecan. Cancer Res 2008;68:9318–22.
19. Nakajima TE, Yasunaga M, Kano Y, et al. Synergistic antitumor activity of the novel SN-38-incorporating polymeric micelles, NK012, combined with 5-fluorouracil in a mouse model of colorectal cancer, as compared with that of irinotecan plus 5-fluorouracil. Int J Cancer 2008;122:2148–53.
20. Simon R, Freidlin B, Rubinstein L, Arbuck SG, Collins J, Christian MC. Accelerated titration designs for phase I clinical trials in oncology. J Natl Cancer Inst 1997;89:1138–47.
21. Matsumura Y, Hamaguchi T, Ura T, et al. Phase I clinical trial and pharmacokinetic evaluation of NK911, a micelle-encapsulated doxorubicin. Br J Cancer 2004;91:1775–81.
22. HA Burris I, Infante JR, Spigel DR, et al. A phase I dose-escalation study of NK012 [abstract 2538]. J Clin Oncol 2008;26.
23. Atsumi R, Suzuki W, Hakusui H. Identification of the metabolites of irinotecan, a new derivative of camptothecin, in rat bile and its biliary excretion. Xenobiotica 1991;21:1159–69.
24. Chu XY, Kato Y, Sugiyama Y. Multiplicity of biliary excretion mechanisms for irinotecan, CPT-11, and its metabolites in rats. Cancer Res 1997;57:1934–8.
25. Takasuna K, Hagiwara T, Hirohashi M, et al. Involvement of β-glucuronidase in intestinal microflora in the intestinal toxicity of the antitumor camptothecin derivative irinotecan hydrochloride (CPT-11) in rats. Cancer Res 1996;56:3752–7.
26. Abigerges D, Chabot G, Armand J, Herait P, Gouyette A, Gandia D. Phase I and pharmacologic studies of the camptothecin analog irinotecan administered every 3 weeks in cancer patients. J Clin Oncol 1995;13:210–21.
27. Matsumura Y, Maeda H. A new concept for macromolecular therapeutics in cancer chemotherapy: mechanism of tumoritropic accumulation of proteins and the antitumor agent smancs. Cancer Res 1986;46:6387–92.
28. Gerrits CJ, de Jonge MJ, Schellens JH, Stoter G, Verweij J. Topoisomerase I inhibitors: the relevance of prolonged exposure for present clinical development. Br J Cancer 1997;76:952–62.
29. Taguchi T, Wakui A, Hasegawa K, et al. Phase I clinical study of CPT-11. Research group of CPT-11. Gan To Kagaku Ryoho 1990;17:115–20.
30. de Forni M, Bugat R, Chabot GG, et al. Phase I and pharmacokinetic study of the camptothecin derivative irinotecan, administered on a weekly schedule in cancer patients. Cancer Res 1994;54:4347–54.
31. Pitot HC, Goldberg RM, Reid JM, et al. Phase I dose-finding and pharmacokinetic trial of irinotecan hydrochloride (CPT-11) using a once-every-three-week dosing schedule for patients with advanced solid tumor malignancy. Clin Cancer Res 2000;6:2236–44.
32. Rothenberg ML, Kuhn JG, Schaaf LJ, et al. Phase I dose-finding and pharmacokinetic trial of irinotecan (CPT-11) administered every two weeks. Ann Oncol 2001;12:1631–41.
33. Haaz MC, Rivory L, Riche C, Vernillet L, Robert J. Metabolism of irinotecan (CPT-11) by human hepatic microsomes: participation of cytochrome P-450 3A and drug interactions. Cancer Res 1998;58:468–72.

Drug Metab. Pharmacokinet. 25 (6): 578–587 (2010).

Regular Article

Genetic Polymorphisms of *FCGRT* Encoding FcRn in a Japanese Population and Their Functional Analysis

Akiko ISHII-WATABE[1,a], Yoshiro SAITO[2,3,b,*], Takuo SUZUKI[1], Minoru TADA[1], Maho UKAJI[2], Keiko MAEKAWA[2,3], Kouichi KUROSE[2,3], Nahoko KANIWA[2,3], Jun-ichi SAWADA[2,4,**], Nana KAWASAKI[1], Teruhide YAMAGUCHI[1], Takako EGUCHI NAKAJIMA[5,†], Ken KATO[5], Yasuhide YAMADA[5], Yasuhiro SHIMADA[5], Teruhiko YOSHIDA[6], Takashi URA[7], Miyuki SAITO[7], Kei MURO[7], Toshihiko DOI[8], Nozomu FUSE[8], Takayuki YOSHINO[8], Atsushi OHTSU[8,9], Nagahiro SAIJO[10,††], Tetsuya HAMAGUCHI[5], Haruhiro OKUDA[2,4] and Yasuhiro MATSUMURA[11]

[1]*Division of Biological Chemistry and Biologicals, National Institute of Health Sciences, Tokyo, Japan*
[2]*Project Team for Pharmacogenetics, National Institute of Health Sciences, Tokyo, Japan*
[3]*Division of Medicinal Safety Sciences, National Institute of Health Sciences, Tokyo, Japan*
[4]*Division of Organic Chemistry, National Institute of Health Sciences, Tokyo, Japan*
[5]*Gastrointestinal Oncology Division, National Cancer Center Hospital, Tokyo, Japan*
[6]*Genetics Division, National Cancer Center Research Institute, National Cancer Center, Tokyo, Japan*
[7]*Department of Medical Oncology, Aichi Cancer Center Hospital, Nagoya, Japan*
[8]*Division of Gastrointestinal Oncology/Digestive Endoscopy, National Cancer Center Hospital East, Kashiwa, Japan*
[9]*Director of Research Center for Innovative Oncology, National Cancer Center Hospital East, Kashiwa, Japan*
[10]*Deputy Director, National Cancer Center Hospital East, Kashiwa, Japan*
[11]*Investigative Treatment Division, National Cancer Center Hospital East, Kashiwa, Japan*
[a,b]*Akiko Ishii-Watabe and Yoshiro Saito contributed equally to this work*

Full text of this paper is available at http://www.jstage.jst.go.jp/browse/dmpk

Summary: Neonatal Fc receptor (FcRn) plays an important role in regulating IgG homeostasis in the body. Changes in FcRn expression levels or activity caused by genetic polymorphisms of *FCGRT*, which encodes FcRn, may lead to interindividual differences in pharmacokinetics of therapeutic antibodies. In this study, we sequenced the 5′-flanking region, all exons and their flanking regions of *FCGRT* from 126 Japanese subjects. Thirty-three genetic variations, including 17 novel ones, were found. Of these, two novel non-synonymous variations, 629G>A (R210Q) and 889T>A (S297T), were found as heterozygous variations. We next assessed the functional significance of the two novel non-synonymous variations by expressing wild-type and variant proteins in HeLa cells. Both variant proteins showed similar intracellular localization as well as antibody recycling efficiencies. These results suggested that at least no common functional polymorphic site with amino acid change was present in the *FCGRT* of our Japanese population.

Keywords: ***FCGRT*; neonatal Fc receptor (FcRn); genetic polymorphism; novel non-synonymous variation**

Received; July 19, 2010, Accepted; September 14, 2010, J-STAGE Advance Published Date; October 1, 2010
**To whom correspondence should be addressed:* Yoshiro SAITO, PhD, *Division of Medicinal Safety Sciences, National Institute of Health Sciences, 1-18-1 Kamiyoga, Setagaya-ku, Tokyo 158-8501, Japan. Tel. +81-3-3700-9528, Fax. +81-3-3700-9788, E-mail: yoshiro@nihs.go.jp*
***Present address: Pharmaceuticals and Medical Devices Agency, Shin-Kasumigaseki Building, 3-3-2 Kasumigaseki, Chiyoda-ku, Tokyo 100-0013, Japan.*
†*Present address: Department of Clinical Oncology, St. Marianna University School of Medicine, 2-16-1 Sugao, Miyamae-ku, Kawasaki-city 216-8511, Japan.*
††*Present address: Kinki University School of Medicine, 377-2 Ohno-Higashi, Osaka-Sayama City, Osaka 589-8511, Japan.*
This study was supported in part by the Program for the Promotion of Fundamental Studies in Health Sciences from the National Institute of Biomedical Innovation, and by the Health and Labor Sciences Research Grants from the Ministry of Health, Labor and Welfare of Japan, and by KAKENHI (20590167) from the Japan Society for the Promotion of Science (JSPS).

Introduction

Neonatal Fc receptor (FcRn) is an immunoglobulin G (IgG) receptor related to major histocompatibility (MHC) class I molecules.[1,2] Like MHC class I, FcRn consists of a heavy chain with extracellular α1, α2, and α3 domains followed by a transmembrane segment and a short cytoplasmic tail and non-covalently bound β2-microglobulin (β2m). FcRn binds the Fc region of monomeric IgG. The FcRn heavy chain is encoded by *FCGRT*, which is located in chromosome 19q13.3 and comprises 6 exons.

In humans, FcRn expression has been observed in a wide variety of tissues including placenta, liver, kidney and vascular endothelium.[1] FcRn has multiple roles in the body such as absorption or secretion of IgG across the intestinal mucosa, and IgG recycling from endothelial cells. With regard to antibody recycling, FcRn binds to the Fc domain of IgG at acidic pH in endosomes after endocytosis, and recycles it back to the extracellular space via the exocytic pathway, thereby protecting IgG from intracellular degradation in lysosomes.[2] This mechanism contributes to the long serum half-life of IgG, and thus, IgG recycling activity is an important function of FcRn and could contribute to the efficacy of antibody therapeutics. Indeed, we previously reported that affinities of antibody therapeutics to FcRn were closely correlated with the serum half-lives reported in clinical studies.[3] The relatively short serum half-life of Fc-fusion proteins such as etanercept, a fusion protein consisting of the extracellular ligand-binding portion of the human tumor necrosis factor receptor linked to the Fc portion of human IgG1, is thought to arise from low affinity to FcRn.[3]

Genetic polymorphisms of genes related to drug metabolism and transport are one of the crucial factors for low-molecular-weight drugs. Pharmacokinetics or pharmacodynamics of biologicals including antibody therapeutics may also be influenced by genetic polymorphisms of transport or target proteins. In this context, changes in FcRn expression levels or activity caused by genetic polymorphisms of *FCGRT* may lead to interindividual differences in pharmacokinetics of antibody therapeutics. However, reports on *FCGRT* genetic polymorphisms in Japanese populations are lacking.

Here we sequenced the 5′-flanking region, all exons and their flanking regions of *FCGRT* from 126 Japanese subjects. We then examined the functional properties of two detected non-synonymous variations using mammalian expression systems focusing on intracellular localization and antibody recycling activities.

Materials and Methods

Human genomic DNA samples: One hundred twenty-six Japanese cancer patients participated in this study. The ethical review boards of the National Cancer Center, Aichi Cancer Center and the National Institute of Health Sciences approved this study. Written informed consent was obtained from all subjects. Genomic DNA for DNA sequencing was extracted from blood leukocytes.

PCR conditions for DNA sequencing: The following sequences obtained from GenBank were used for primer design and reference sequences: NW_927240.1 (genome) and NM_004107.3 (mRNA). For sequencing, two sets of long-range PCR were performed to amplify all 6 exons from 50 ng of genomic DNA with two sets of primers (0.5 μM) designed in the promoter or intronic regions as listed in "1st PCR" of **Table 1**. We used LA-Taq with GC buffer I (0.05 U/μl, Takara Bio Inc., Shiga, Japan) to amplify from the 5′-flanking region to exon 3 and Z-Taq (0.025 U/μl, Takara Bio. Inc.) from exons 4 to 6, as described in **Table 1**. The 1st PCR conditions were 94°C for 5 min, followed by 30 cycles of 94°C for 30 sec, 60°C for 1 min, and 72°C for 2 min, and then a final extension at 72°C for 7 min for LA-Taq, and 30 cycles of 98°C for 5 sec, 55°C for 5 sec, and 72°C for 190 sec for Z-Taq. Next, each region was separately amplified in the 2nd PCR using the 1st PCR product as the template. We used LA-Taq with GC buffer I or II (0.05 U/μl) for amplifying regions from the 5′-flanking region to exon 3 and Ex-Taq (0.02 U/μl, Takara Bio. Inc.) from exons 4 to 6 as described in **Table 1**. The 2nd PCR conditions were 94°C for 5 min, followed by 30 cycles of 94°C for 30 sec, 60°C for 1 min, and 72°C for 2 min, and then a final extension at 72°C for 7 min for all regions. The PCR products were then treated with a PCR Product Pre-Sequencing Kit (USB Co., Cleveland, OH, USA) and directly sequenced on both strands using an ABI BigDye Terminator Cycle Sequencing Kit ver. 3.1 (Applied Biosystems, Foster City, CA, USA) and the sequencing primers listed in **Table 1** (Sequencing). Excess dye was removed by a DyeEx96 kit (Qiagen, Hilden, Germany) and the eluates were applied to an ABI Prism 3730xl DNA Analyzer (Applied Biosystems). All relatively low frequent variations ($n \leq 5$) were confirmed by repeated sequencing analyses of PCR products generated from original (not amplified) genomic DNA. The nucleotide positions based on the cDNA sequence were numbered from the adenine of the translational initiation site or the nearest exons.

Hardy-Weinberg equilibrium and linkage disequilibrium (LD) analyses: Hardy-Weinberg equilibrium and LD analyses were performed by SNPAlyze software ver. 7 (Dynacom Co., Yokohama, Japan). Hardy-Weinberg equilibrium was assessed by the $\chi 2$ test and pairwise LDs between variations were obtained for the frequently used coefficients $|D'|$ and rho square (r^2). $|D'|$ is used to assess the probability for past recombinations, and r^2 is used as a parameter for the linkage between a pair of variations.

Table 1. Primers used for sequencing *FCGRT*

	Enzyme*	Amplified or sequenced region	Forward primer (5′ to 3′)	Reverse primer (5′ to 3′)	Amplified length (bp)
1st PCR	LA-GI	5′-flanking to Exon 3	CTCAGGCTGGTCCTTGAACTCA	ATTAGCCAGTTATGGTGGTATG	5,244
	Z	Exons 4 to 6	CAAGTGTGGTGGTGGGCACCTA	GGGAGTTCGAGACCAGCCTGAT	3,788
2nd PCR	LA-GI	5′-flanking	CTGAACCAGCTGAACGTCCACT	CTGAGCGTGGTGGTGGGCCTGT	1,058
	LA-GII		ATAGAGGTGACAGTTGCACAGC	GGTCCAGACTGACAACAATGCC	1,477
	LA-GII	Exon 1	GAGCAGCAGCCTCCCACAGGAT	ACACAAGAGGCGACAGGTGGTT	1,017
	LA-GI	Exons 2 to 3	ATTGTTGTCAGTCTGGACCG	GCTGCAGTGGGAGGCTGATGGA	1,332
	Ex	Exons 4 to 5	CCAAGGAGGTGACATCTTGAGG	CATCTCTGGGTTTCTGTCTCCA	1,383
	Ex	Exon 6	CCGCCTTGCCGCTGCTGATCCA	GAGCTGAGATCACGCAATTGTA	1,632
Sequencing		5′-flanking	CTGAACCAGCTGAACGTCCACT	CAGGGTCTGGCTCTGTCACTCA	
			GTGCAGAATAGGCAAATCTATC	AACCACATCCTTCTGCTAGGAC	
			CGGGTTCAAGCAATTCTCCTGT	TTGAGGGTGTCTGCCGCTCAGG	
			GAGCAGCAGCCTCCCACAGGAT	CCTCCTCTCTCAGACCCAGGAA	
			CCTGGGTCTGAGGGAGGAGT	CCTCCTCGTACCTGAAGAACTT	
		Exon 1	GGACTCTCAGCCTATCAAGT	ACACAAGAGGCGACAGGTGGTT	
			CCGCGGTGTCCCGGGAGGAA		
		Exons 2 to 3	GTATCTGTCCCACTGCAGTCTA	AACTGAGGCAGGTGGGCATGAC	
		Exon 4	TGAGTCTCTGTCACCTAGGAAG	AGTTAACAGCTCTTCAGACTCA	
		Exon 5	CCGCCTTGCCGCTGCTGATCCA	GTCTCTGTCCTCCCAGGTCTGT	
		Exon 6	TCAGAGAGAGGTGGAGACAGAA	GATGTATAAAACTGGCAGGTTC	
			CCTTGGATCTCCCTTCGTGGAG	TGGCTCACACTTGTAATCCCAC	
			GACGGAGTCTTGCTCTGTTGCT		

*LA-GI: LA-Taq with GC buffer I, LA-GII: LA-Taq with GC buffer II, Z: Z-Taq, Ex: Ex-Taq.

Construction of FcRn expression plasmid: Wild-type human FcRn cDNA was originally obtained from pME18SFL3 (AK075532) (Toyobo, Osaka, Japan). The coding region of FcRn cDNA subcloned into pcDNA3 was amplified by PCR, and then inserted into the EcoRI/SalI site of pEGFP-(C) plasmid. The resulting plasmid encodes hFcRn with C-terminally fused enhanced green fluorescent protein (EGFP) containing the eight amino acid-linker peptide VDSRGSRV between the two proteins. Mutations were introduced by an inverse PCR method. Primers consisted of 5′-AAG GCC CAA CCC AGC AGC CCT GGC TTT-3′ (forward) and 5′-CAG GCG CAT GGA GGG GGG CC CTT CCA-3′ (reverse) for R210Q, 5′-TCC ACC GTC CTC GTG GTG GGA ATC GTC-3′ (forward) and 5′-CTT GGC TGG AGA TTC CAG CTC CAC CCT-3′ (reverse) for S297T. The underlines indicate the mutated nucleotides. The variant plasmids were sequenced on both strands for the entire cDNA region to confirm the introduction of the mutation only at the target sites. Human β2 microglobulin (β2m) cDNA was obtained from pME18SFL3 (FCC106E07) (Toyobo). β2m cDNA was subcloned into pcDNA3.1/
Hygro. The β2m construct was used because FcRn becomes a heterodimer with β2m, which is necessary for the proper intracellular localization of FcRn.[4,5]

Cell culture and plasmid transfection: HeLa cells were cultured in DMEM (Sigma-Aldrich, St. Louis, MO, USA) supplemented with 10% fetal calf serum (Nichirei, Tokyo, Japan). The plasmids encoding the wild-type or variant FcRn fused with EGFP along with the plasmid encoding β2m were transfected into HeLa cells using Lipofectamine 2000 reagent (Invitrogen, Carlsbad, CA, USA) according to the manufacturer's protocol. Plasmids encoding wild-type or variant FcRn fused with EGFP were used for all experiments, including the intracellular localization and antibody recycling activity of FcRn.

Western blot analysis: Wild-type and variant FcRn-EGFP transfected into HeLa cells in 35-mm-diameter dishes were lysed with 500 μL of RIPA buffer [50 mM Tris HCl (pH 7.6), 150 mM NaCl, 1% Nonidet P-40 and 0.25% sodium deoxycholate] supplemented with protease inhibitors (Nacalai Tesque, Kyoto, Japan). After incubation on ice for 30 min, the lysates were centrifuged at 15,000 rpm at 4°C for 20 min. An aliquot (3 μL) of the supernatant was diluted in SDS-sample buffer and applied to 10% SDS-polyacrylamide gel. After electrophoresis, separated proteins were transferred onto polyvinylidene fluoride membrane. Immunochemical detection of FcRn-EGFP proteins was performed using rabbit anti-human FcRn antibody raised against a peptide antigen (residues 135–148, LNGEEFMNFDLKQG). Visualization of the proteins was achieved with horseradish peroxidase-conjugated anti-rabbit IgG antibody (Cell Signaling Technology, Danvers, MA, USA) and the ECL Plus Western blotting detection reagent (GE Healthcare Bio-Sciences AB, Uppsala, Sweden). Protein band densities measured by LAS-3000 (Fuji Film, Kanagawa, Japan) were quantified with Multi Gauge software (Fuji Film).

The relative expression levels are shown as means ± SD of three separate transfection experiments. To verify that the samples were evenly loaded, the blot was reprobed with anti-glyceraldehyde-3-phosphate dehydrogenase (G3PDH) antibody (R&D Systems, Minneapolis, MN, USA).

Fluorescent labeling of antibodies: As a model antibody, we used infliximab, a clinically used chimeric anti-human TNFα antibody which has the Fc domain of human IgG1. The binding of infliximab to human FcRn was shown by surface plasmon resonance analysis in our previous study.[3] Infliximab, kindly provided by Tanabe Pharmaceutical Co. Ltd. (Osaka Japan), was labeled with CypHer5 (GE Healthcare Bio-Sciences, Uppsala, Sweden) by incubating with CypHer5E mono NHS ester in PBS containing 0.5 M Na_2CO_3 (pH 8.3) for 1 hr at room temperature. After the reaction, unbound dye was removed by dialysis in PBS. The protein concentration and degree of labeling were determined by spectrophotometry. IgY (Jackson Immuno Research Laboratories, West Grove, PA, USA) was also labeled with CypHer5 and used in control experiments.

Imaging with fluorescence microscopy: HeLa cells transfected with wild-type or variant FcRn-EGFP cDNA and the β2m cDNA were cultured on 35-mm poly-L-lysine-coated glass-bottom dishes (0.08–0.12 mm thickness) (Matsunami, Osaka, Japan) for 2–4 days. The intracellular localization analyses of wild-type and variant FcRn-EGFP were carried out by confocal laser scanning fluorescence microscopy using a Carl Zeiss LSM510 system (Carl Zeiss, Jena, Germany). For co-localization experiments, wild-type or variant FcRn-EGFP-transfected HeLa cells were incubated with CypHer5-labeled infliximab diluted in cell culture medium containing 200 mM sodium phosphate buffer (pH 6.0) for 2–3 hr at 37°C. Note that throughout this study, the cell culture media used for incubation with the labeled antibody was acidified (pH 6.0) to obtain enhanced incorporation of antibodies into the cells, as reported previously.[6,7] The fluorescent signal was observed in neutral pH medium after washing the cells twice. The 488- and 633-nm laser lines were used to image FcRn-EGFP and CypHer5 labeled-infliximab, respectively.

Biotin labeling of antibodies: Infliximab and IgY were labeled with biotin using EZ-link sulfo-NHS-biotin (Pierce, Rockford, IL, USA). Antibodies and sulfo-NHS-biotin were mixed at the molar ratio of 1:20 and incubated for 60 min at room temperature. Biotinylated antibodies were purified using Zeba desalt spin column (Pierce). Protein concentration was determined by BCA protein assay (Pierce) using bovine serum albumin as a standard.

Recycling assay: HeLa cells were transfected with the wild-type or variant FcRn-EGFP construct along with the β2m construct. The day after transfection, cells were seeded on 96-well plates at 4×10^4 cells/well. After further culturing for one day, recycling assays were performed. Hanks' balanced salt solutions (HBSS) (pH 6.0 and 7.4) were prepared supplemented with 10 mM MES (pH 6.0) and 10 mM Hepes (pH 7.4). The cells were washed with HBSS (pH 7.4) and pre-incubated with HBSS (pH 7.4) for 30 min at 37°C. After washing with HBSS, 10 μg/ml of biotinylated infliximab diluted in HBSS (pH 6.0) containing 0.5% fish gelatin was added to each well. The cells were incubated at 37°C for 1 hr to allow the antibody to be incorporated into the cells. Cells were then washed five times with HBSS (pH 7.4). Then, HBSS (pH 7.4) supplemented with 2% ultra-low IgG FCS (Invitrogen) was added to each well and incubated at 37°C for the indicated periods of time. The supernatant was collected and subjected to ELISA for quantitating the recycled antibody. In order to determine the amount of biotinylated infliximab incorporated into the cells during the 1-hr incubation at 37°C, cells were lysed using RIPA buffer supplemented with protease inhibitors (Nacalai Tesque, Kyoto, Japan) after washing five times with HBSS, and the lysate was subjected to ELISA. Biotinylated IgY was also used as a negative control in some experiments.

Enzyme linked immunosorbent assay (ELISA) for biotinylated antibody: NeutrAvidin (Pierce, Rockford, IL) was bound on Maxisorp 96-well black plates (Thermo Fisher Scientific, Roskilde, Denmark) using IMMUNO-TEK ELISA construction system (ZeptoMetrix, Buffalo, NY, USA). Supernatants or lysates obtained from the recycling assay were applied on the wells and incubated for 16 hr at 4°C. The plates were washed three times with Tris-buffered saline (pH 7.6) containing 0.1% Tween-20 (TBST). Peroxidase-conjugated goat anti-human IgG (Pierce) diluted with TBST was added to the plate and incubated for 1 hr at room temperature. After washing three times with TBST, chemiluminescent reagent (SuperSignal ELISA Femto, Pierce) was added and incubated for 1 min at room temperature. The chemiluminescent signal was detected using an ARVO 1420 multilabel counter (Perkin Elmer, Waltham MA, USA). When the amount of biotinylated IgY was measured, peroxidase-conjugated rabbit anti-chicken IgY (Promega, Madison, WI, USA) was used. For generation of a standard curve, 0.1 to 10 ng/ml of biotinylated corresponding protein was used.

Results

***FCGRT* variations found in a Japanese population:** Thirty-three genetic variations were found, including 17 novel ones, in 126 Japanese subjects (**Table 2**). Of these variations, 14 were located in the 5′-flanking region, 4 (2 synonymous and 2 non-synonymous) in the coding exons, 13 in the introns, 1 in the 3′-untranslated region (UTR), and 1 in the 3′-flanking region. All detected variations were in Hardy-Weinberg equilibrium

Table 2. Summary of *FCGRT* variations detected in this study

SNP ID		Location	Position		Nucleotide change	Amino acid change or known VNTR	Frequency	
This Study	dbSNP (NCBI) or reference		NW_927240.1	From the translational initiation site or from the end of the nearest exon				95% Confidence interval
MPJ6_FRT001[a]		5′-flanking	1557122	−2230	agaacctgaactA>Ccctgaccagcag		0.004	0.000–0.012
MPJ6_FRT002[a]			1557195	−2157	gggtgtcttgcaC>Actgtcatcccag		0.008	0.000–0.019
MPJ6_FRT003	rs78889190		1557207	−2145	cctgtcatccccaG>Ctgctttgggagg		0.020	0.003–0.037
MPJ6_FRT004[a]			1557221	−2131	gctttgggaggcC>Taaggtgggaggc		0.004	0.000–0.012
MPJ6_FRT005[a]			1557498_1557505	−1854_−1847	ggaaggaaggaaGGAAGGAA/-ggaggcaaggaa		0.024	0.005–0.043
MPJ6_FRT006	rs60964075		1557502_1557505	−1850_−1847	ggaaggaaggaaGGAA/-ggaggcaaggaa		0.103	0.066–0.141
MPJ6_FRT007	rs60964075		1557505_1557506	−1847_−1846	ggaaggaaggaaggaa-/GGAAggaggcaaggaa		0.099	0.062–0.136
MPJ6_FRT008[a]			1557505_1557506	−1847_−1846	ggaaggaaggaaggaa-/GGAAGGAAggaggcaaggaa		0.020	0.003–0.037
MPJ6_FRT009[a]			1557506	−1846	ggaaggaaggaaG>Agaggcaaggaag		0.004	0.000–0.012
MPJ6_FRT010[a]			1557540_1557547	−1812_−1805	aaggaaggaaggAAGGAAGG/-aggcaaggaagg		0.004	0.000–0.012
MPJ6_FRT011	rs2335534		1557671	−1681	tctgggagcagcG>Agctgtttaacgg		0.028	0.007–0.048
MPJ6_FRT012[a]			1558366	−986	gatacagagggT>Gaggaggaggatc		0.004	0.000–0.012
MPJ6_FRT013	ref. 8		1558963_1558999	−389_−353	cgagggtagagcGGTTGGGGGCCCGGACTCCTGG GTCCGAGGGTAGAGC/-ggttgggggccc	VNTR3>VNTR2	0.032	0.010–0.053
MPJ6_FRT014[a]			1559173	−179	actgagatccagT>Gtcaggggtgaaa		0.028	0.007–0.048
MPJ6_FRT015	rs59774409	Intron 1	1559442	IVS1+18	ggccgctccgggC>Tcagggccctgct		0.028	0.007–0.048
MPJ6_FRT016[a]			1559453	IVS1+29	gccagggccctgC>Ttgcaggcgggcg		0.147	0.103–0.191
MPJ6_FRT017	rs11551281	Exon 2	1559885	126[b]	ctcgcctgccccgG>Tgggactcctgcc	Pro42Pro	0.044	0.018–0.069
MPJ6_FRT018	rs2878342	Exon 3	1560418	582[b]	ggagaggggccgC>Tggaaacctggag	Arg194Arg	0.028	0.007–0.048
MPJ6_FRT019[a]		Exon 4	1570485	629[b]	gcctgaaggcccG>Aacccagcagccc	Arg210Gln	0.004	0.000–0.012
MPJ6_FRT020	rs3810194	Intron 4	1570734	IVS4+7	agctgggtgaggT>Cccgccaggtgg		0.048	0.021–0.074
MPJ6_FRT021	rs1132990		1570857	IVS4+130	gccttgaacctcA>Gcgcctgtcagtg		0.048	0.021–0.074
MPJ6_FRT022[a]			1570915	IVS4+188	ccaactgccttcC>Tgtctcctgctgc		0.020	0.003–0.037
MPJ6_FRT023	rs10525267		1571020_1571025	IVS4+293_+298	tgctgctgctgcTGCTGC/-gggtcttcctgg		0.083	0.049–0.117
MPJ6_FRT024[a]			1571170	IVS4–238	ctggcacagcccC>Tgccttgccgctg		0.020	0.003–0.037
MPJ6_FRT025	rs73582442		1571235	IVS4–173	gctggttcttacG>Atccaacctgggg		0.048	0.021–0.074
MPJ6_FRT026	rs73582446		1571314	IVS4–94	gctggaatctccG>Aaggctgggaggg		0.048	0.021–0.074
MPJ6_FRT027[a]		Exon 5	1571425	889[b]	ccagccaagtccT>Accgtgctcgtgg	Ser297Thr	0.020	0.003–0.037
MPJ6_FRT028	rs55662447	Intron 5	1571614_1571615	IVS5+90_+91	agagacccagagAG/-gggggacagaga		0.028	0.007–0.048
MPJ6_FRT029[a]			1571615	IVS5+91	gagacccagagaG>Tgggggacagaga		0.004	0.000–0.012
MPJ6_FRT030	rs77741672		1571691	IVS5+167	gagaggggacgG>Cagacagagaccc		0.151	0.107–0.195
MPJ6_FRT031[a]			1571915	IVS5–46	gtcagacccagaG>Acgcctcagagat		0.020	0.003–0.037
MPJ6_FRT032	rs14769	3′-UTR	1572276	1304 (*206)[c]	taacacgagtttG>Aggcccgaatcag		0.044	0.018–0.069
MPJ6_FRT033[a]		3′-flanking	1572364	1312+80 (*214+80)[d]	tgggcctcggatC>Ttctcctacaggt		0.004	0.000–0.012

[a]Novel variations detected in this study.
[b]Positions in cDNA (NM_004107.3).
[c]Numbered from the termination codon TGA.
[d]Positions were shown as 1312 (*214) (final base of exon 6)+bases from the end of exon 6.